What's important for sex

A Thesis

submitted to

Indian Institute of Science Education and Research Pune in partial fulfilment of the requirements for the BS-MS Dual Degree Program

by

Nandeesh Sharma

Indian Institute of Science Education and Research Pune

Dr. Homi Bhabha Road,

Pashan, Pune 411008, INDIA.

Date: March 16, 2025

Under the guidance of

Supervisor: **Dr SaraH E. Zanders**,

Stowers Institute for medical Research

From June 2024 to March 2025

INDIAN INSTITUTE OF SCIENCE EDUCATION AND RESEARCH PUNE

Certificate

This is to certify that this dissertation entitled "**What's important for sex**" towards the partial fulfilment of the BS-MS dual degree program at the Indian Institute of Science Education and Research, Pune represents study/work carried out by **Nandeesh Sharma** at **Stowers Institute for Medical Research** under the supervision of **Dr SaraH E. Zanders**, Associate Investigator during the academic year 2024-2025.

Dr SaraH E. Zanders

Committee:

Dr. SaraH E. Zanders (Supervisor)

Dr. Mridula Nambiar (TAC member)

This thesis is dedicated to my parents and sisters

Declaration

I hereby declare that the matter embodied in the report entitled "**What's important for sex**" are the results of the work carried out by me at the **Stowers Institute for Medical Research**, under the supervision of **Dr SaraH E. Zanders**, and the same has not been submitted elsewhere for any other degree. Wherever others contribute, every effort is made to indicate this clearly, with due reference to the literature and acknowledgement of collaborative research and discussions.

Nandeesh Sharma

20201027

Table of Contents

List of figures

List of tables

Abstract

Sexual reproduction is one of the key features of eukaryotic organisms, essential for survival and evolution of most species. Although the mechanisms of sexual reproduction are largely conserved across all eukaryotes, our understanding of the molecular machinery governing sexual reproduction remains incomplete. This study examines the role of *ifs1* in sexual reproduction using fission yeast *Schizosaccharomyces pombe* as the model system. *ifs1* was identified as one of the hits of a genetic screen to identify all the genes contributing to sexual reproduction in fission yeast. I have utilized fluorescence microscopy to study the involvement of *ifs1* in different stages of sexual reproduction and found that *ifs1* is required for the formation of a functional spore wall. *ifs1*Δ mutants form spores with an irregular morphology and very low viability. I have used electron microscopy to reveal that the *ifs1*Δ mutants form a weak spore wall with non-uniform thickness. Spores lacking *ifs1* form a bud-like outgrowth on the surface, which enlarges till the spore wall ruptures, allowing the cytoplasmic material to escape. I characterized the composition of the spore wall using FTIR spectroscopy and found that *ifs1* is required for β-glucan assembly in the spore wall. In addition, I have engineered single-site mutants of Ifs1 protein to characterize its biochemical activity and have revealed that the highly conserved pyrophosphatase domain of Ifs1 is not required for its role in spore wall formation. Furthermore, my data suggest fission yeast spore walls have three layers, as opposed to the previously hypothesized two-layer model.

Acknowledgement

The number of people I would like to acknowledge here will definitely exceed the word limit. I will start off by thanking SaraH for taking me in as a student and giving me the opportunity to work on this cool project. I will miss our weekly discussions, coming up with innovative ideas and cursing over the unsuccessful results. Thank you for guiding me throughout the project and providing a direction to my efforts.

I would also like to thank the all the Zanders lab members for helping me with my experiments and providing constructive insights towards my project. I will miss all the philosophical and not so philosophical lunch discussions we had on the most random and peculiar topics. I am grateful to everyone for providing a welcoming and fun work environment. I appreciate Andy for mentoring me and bearing with my naive questions and mistakes.

Jeff helped me with the confocal microscopy and FTIR-spectroscopy experiments. I appreciate all the ideas and help he provided with the experiments. Steph helped me a lot with electron microscopy and designing experiments to get the best images. I definitely couldn't have completed my thesis if she didn't push forward my samples despite her busy schedule.

I am grateful to my friends for keeping me sane during my project and my time at IISER. I am indebted to all the associates and unlawful residents of 231 for the never-ending supply of troubles and mishaps. Thank you for not letting me have a simple and mundane life.

Lastly, I would like to thank my family for accepting my atypical career choices. I am thankful to my parents for supporting me and making me capable of taking my own decisions and facing any difficulty. I am thankful to my sisters for being cruel and making me self-reliant.

Contributions

Contributor name	Contributor role
Nandeesh Sharma, Dr SaraH Zanders	Conceptualization Ideas
Nandeesh Sharma, Dr SaraH Zanders, Jeff Lange, Stephanie Nowotarski	Methodology
–	Software
Nandeesh Sharma	Validation
Nandeesh Sharma	Formal analysis
Nandeesh Sharma, Jeff Lange, Stephanie Nowotarski	Investigation
Dr SaraH Zanders	Resources
Nandeesh Sharma	Data Curation
Nandeesh Sharma	Writing - original draft preparation
Nandeesh Sharma, Dr SaraH Zanders	Writing - review and editing
Nandeesh Sharma	Visualization
Dr SaraH Zanders	Supervision
Dr SaraH Zanders	Project administration
Dr SaraH Zanders	Funding acquisition

Introduction

1. Sexual Reproduction

Sexual reproduction is a fundamental aspect of life cycle in most eukaryotes. It is broadly conserved and depends on the formation of specialized cells called gametes. Gametes are haploid cells formed by meiosis, which fuse to form a diploid zygote. The zygote, in turn, undergoes multiple mitotic cycles to develop into an adult organism. Sexual reproduction increases the genetic diversity in a population, ultimately promoting variation and increasing the chances of survival (Alberts *et al.*, 2002). Despite its ubiquitous nature and importance in survival of species over long evolutionary timescales, the molecular mechanisms underlying sexual reproduction are not completely understood even in well-studied organisms. We have employed *Schizosaccharomyces pombe* as a model system to study the mechanisms governing sexual reproduction and identify the role of genes contributing to sexual health.

2. Fission yeast

Fission yeast *Schizosaccharomyces pombe* is a simple, unicellular fungi, which has been widely used as a model organism for studying molecular and cellular biology of eukaryotic cells owing to its genetic tractability and fundamental cellular processes homologous to advanced eukaryotes such as mammalian cells (Hoffman *et al.*, 2015).

2.1 Life cycle of fission yeast

S. pombe exists in a haploid state under normal environmental conditions and propagates vegetatively by mitosis. However, it responds to nitrogen starvation by employing to sexual reproduction and formation of spores (Hoffman et al., 2015; Vyas et al., 2021). The process of sporulation in fission yeast mainly consists of 3 steps -

conjugation between cells of opposite mating types to form a diploid, meiosis to form prespores and formation of spore envelope to form a mature spore (Fig. 1).

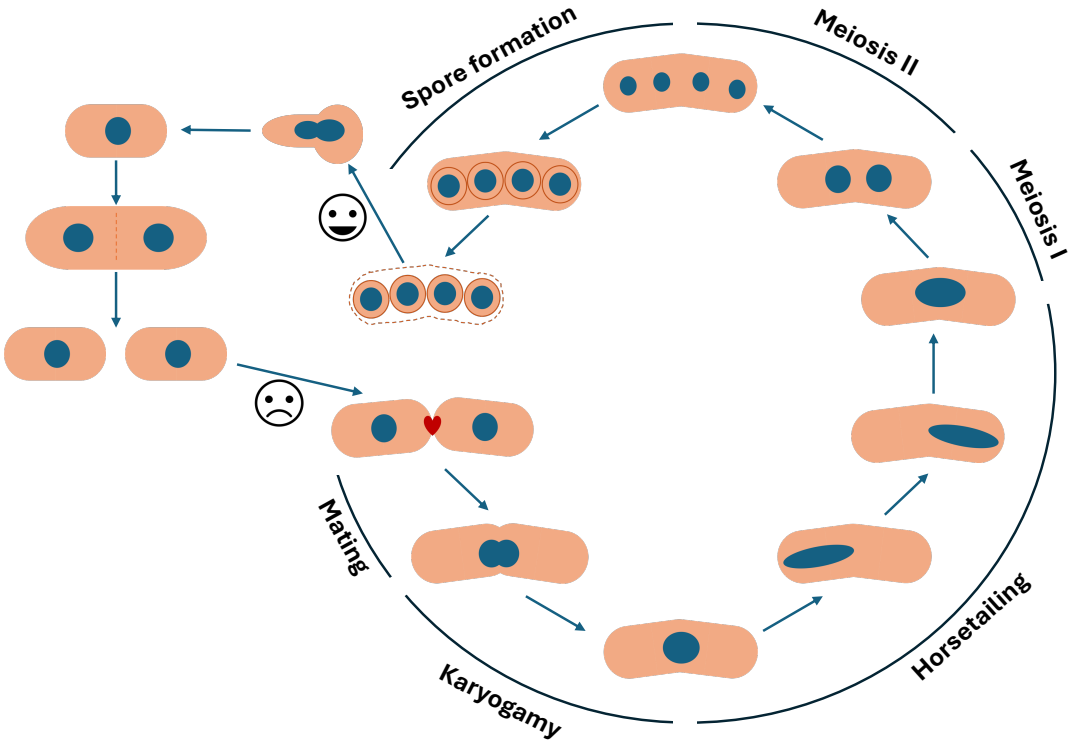

Figure 1: Life cycle of fission yeast

The haploid cell divides vegetatively by mitosis under normal environmental conditions. However, when introduced to a nitrogen deprived environment, two compatible haploid cells mate to form a diploid, which undergoes meiosis to produce four haploid spores in an ascus. The ascus eventually breaks down, and the spores germinate in a glucose-rich environment to form haploid daughter cells.

Mating

Fission yeast has two distinct mating types which can mate with each other. The mating type is determined based on the allele expressed at the mating type locus present on chromosome 2. The *mat* locus is composed of three genes– *mat1, mat2-P* and *mat3-M* (Leupold, 1958; Egel and Gutz, 1981). The *mat2* and *mat3* are silent

cassettes which can move their genetic information to the active *mat1* locus by a recombination event to regulate the active mating type (Beach and Klar, 1984). The heterothallic strains have either *mat2-P* (h^+) or *mat2-M* (h^-) loci transcriptionally active and can effectively mate only with the opposite mating type. The homothallic strain (h^{90}) has both the *mat2-P* and *mat3-M* regions and can undergo mating type switch and mate within the same culture (Egel, 1977; Miyata and Miyata, 1981; Egel *et al.*, 1984). The vegetative cells exit the cell cycle in response to nitrogen starvation and enter a quiescent state. In presence of a mating partner, the vegetative cell enters the sexual cycle and undergoes mating. Mating involves conjugation of cells of opposite mating type and fusion of nuclei to form a diploid cell. The diploid nucleus soon enters the meiotic cycle to form four haploid nuclei (Fig. 1).

Meiosis

Once a diploid cell is formed, it immediately enters meiosis in a nitrogen starved environment, ensuring spore formation. Meiosis in *S. pombe* involves a series of meiosis-specific genes, which facilitates homologous recombination and other meiotic pathways. These include specialized recombination proteins, meiosis-specific chromosome scaffolding factors, kinetochore complex proteins and cohesion proteins that link sister chromatids (Hunter, 2015; Lam and Keeney, 2015). The diploid nucleus undergoes DNA synthesis and undergoes a nuclear “horsetail” movement to reorganize and facilitate homologous pairing and recombination. (Fig. 1)(Yamamoto *et al.*, 1999). During Prophase I, the spindle pole body (SPB) undergoes remodeling and embeds into the nuclear envelop in meiosis I to function as a microtubule-organizing center (MTOC), forming spindles and regulating chromosome segregation (Shimoda, 2004). Four haploid nuclei are formed at the end of the two meiotic divisions (Fig. 2).

Spore envelope formation

The spore envelope consists of the forespore membrane (FSM) and the spore cell wall. The spindle pole body undergoes modification to form meiotic outer plaques (MOPs) during prophase II which serves as a platform for de novo forespore membrane assembly (Fig. 2) (Shimoda, 2004; Ohtsuka *et al.*, 2022a). During meiosis II, vesicles derived from various intracellular organelles including endoplasmic reticulum, vacuoles, plasma membrane and Golgi accumulate to the meiotic outer plaques with the help of Rab protein cascade to form a forespore membrane precursor (Imada and Nakamura, 2016).

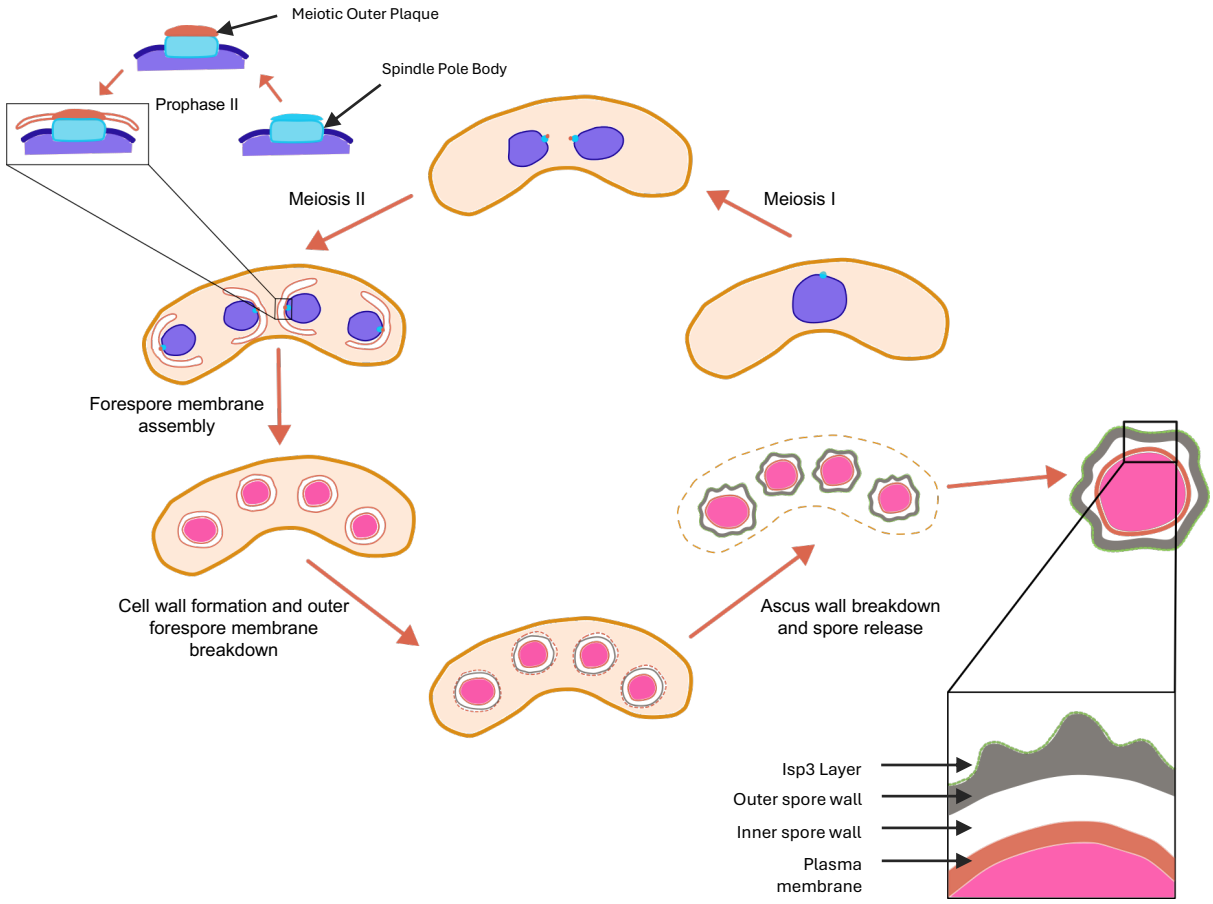

Figure 2: Spore formation and spore envelope maturation in fission yeast

During prophase II, the spindle pole body undergoes modification to form meiotic outer plaques (MOPs) which serves as a platform for de novo forespore membrane assembly. The

forespore membrane is a double-layered structure, which expands to encapsulate the haploid nucleus, and the spore wall assembles between the two membranes. This is followed by the deposition of Isp3 protein coat outside the spore wall. The outer forespore membrane breaks down eventually and the inner forespore membrane serves as the plasma membrane of mature spores. Mature spores are released with the endolysis of ascus cell wall. Enlarged view of spore envelope showing Isp3 coat, outer and inner spore wall and the plasma membrane.

SNARE proteins drive the fusion of vesicles and membrane, required for forespore membrane assembly and expansion (Nakamura *et al.*, 2001; Shimoda, 2004; Yamaoka *et al.*, 2013). Proper forespore membrane expansion requires leading edge proteins (LEPs), which form a ring structure at the leading front of the expanding membrane (Okuzaki *et al.*, 2003; Shimoda, 2004; Nakamura-Kubo *et al.*, 2011; Ohtsuka *et al.*, 2022a) At the end of meiosis II, the spindle pole body extrudes out from the nuclear envelope and reverts to the original form. The face of the spindle pole bodies towards the ascal cytoplasm i.e., the meiotic outer plaque disassembles, and the forespore membrane separates from the nuclear envelope (Hirata and Shimoda, 1994; Shimoda, 2004). The forespore membrane is a double-layered membrane which encloses the haploid nucleus to form a prospore (Fig. 2). The spore wall assembles between the two membranes and the outer FSM degrades shortly after. The inner forespore membrane develops into the plasma membrane of the mature spore.

Spore germination

Mature spores are released into the environment with the endolysis of the ascus cell wall by the endo-β-1,3-glucanase Eng2 and endo-α-1,3-glucanase Agn2, which localize in the cytoplasm of the ascus (Fig. 2)(Dekker *et al.*, 2007; Encinar Del Dedo *et al.*, 2009).

When introduced to a glucose-rich environment, the spores exit dormancy and resume metabolic activities to re-enter mitotic cycle (Hatanaka and Shimoda, 2001). Germinating spores undergo polarized growth and division to form vegetative haploid cells (Fig. 1). Germination proceeds by increase in cell size with localized rupture of outer spore wall to form a polar cap (Bonazzi *et al.*, 2014; Tahara *et al.*, 2020). A projection emerges from the swollen spore called an outgrowth to form a 'pear'-shaped cell, which extends progressively opposite to the spore side. The nucleus divides and the polarized tube separates from the spore mother cell to form a vegetative daughter cell (Bonazzi *et al.*, 2014).

2.2 Cell wall

The cell wall is the rigid outermost layer which provides resistance against mechanical stress and is also responsible for maintaining cell shape. The cell wall of fission yeast essentially consists of several polysaccharides including glucans, galactomannans and chitin (Fig. 3) (Free, 2013; Gow *et al.*, 2017). Earlier studies using transmission electron microscopy have revealed that the cell wall of *S. pombe vegetative cells* has three layers – electron-dense inner and outer layer and an electron-transparent middle layer. The dark inner and outer layers are composed of galactomannans, whereas the middle layer is mainly composed of α and β-glucans (Fig. 3)(Horisberger *et al.*, 1978). The glucans are the main components, with β-glucans and α-glucans accounting for 54-60% and 28-32% of the total cell wall respectively (Pérez *et al.*, 2018).

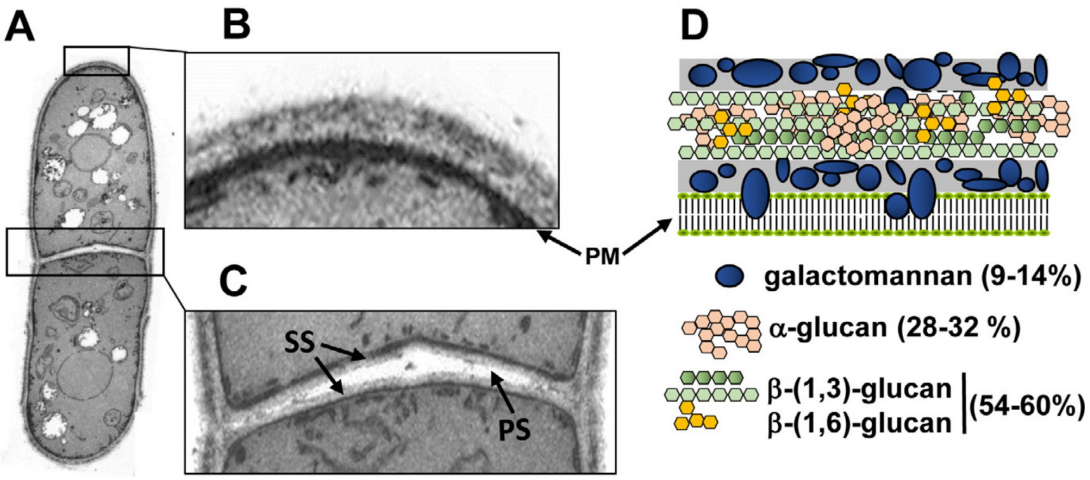

Figure 3: Cell wall of fission yeast

(A) Transmission electron micrograph of *S. pombe* cell vegetative cell. Zoomed in view of (B) the cell wall and (C) septum are shown. (D) Schematic diagram representing organization of cell wall of fission yeast vegetative cell. PM: Plasma membrane, SS: Secondary septum, PS: primary septum. (figure adapted from Pérez *et al.*, 2018)

β-glucan

The β-glucan is a polymer of D-glucose linked by β-(1,3) and β-(1,6) bonds. It is divided into three categories on the basis of type on bonding of the main chain: linear β-(1,3)-glucan, branched β-(1,3)-glucan, and branched β-(1,6)-glucan (Manners and Meyer, 1977; Pérez *et al.*, 2018). β-(1,3)-glucan is the major structural component which forms a network of fibers deposited onto the plasma membrane to cover the whole surface (Osumi *et al.*, 1998; Humbel *et al.*, 2001; Muñoz *et al.*, 2013). β-(1,3)-glucan is synthesized at the cell surface by β-(1,3)-glucan synthase enzyme (Ishiguro *et al.*, 1997; Liu *et al.*, 1999; Jin and McCollum, 2003). The enzyme has two subunits – a catalytic subunit encoded by the *bgs* genes (*bgs1,bgs2,bgs3 and bgs4*) and the regulatory subunit, small GTPase Rho1 (Arellano *et al.*, 1996; Liu *et al.*, 1999,2000; Martín *et al.*, 2000, 2003; Cortés *et al.*, 2005). GPI-bound Gas proteins further

elongate and branch the newly synthesized β-(1,3)-glucan chains (Ragni *et al.*, 2007; De Medina-Redondo *et al.*, 2010).

α-glucan

α-glucan is a polysaccharide made of linear chains of D-glucose linked by α-(1,3) bond, with two chains connected via α-(1,4) bond at the reducing end (Grun, 2004). It colocalizes with the β-glucan and is essential for the rigidity of the cell wall (Cortés *et al.*, 2012). α-glucan is synthesized by Ags1 (Mok1) in vegetative cells and is found on growing poles and septa (Hochstenbach *et al.*, 1998).

Galactomannan

Galactomannan constitutes the glycan part of cell wall glycoproteins. It is a branched polymer of D-mannose with a D-galactose residue at the non-reducing end (Peat *et al.*, 1961). It is essential for the adherence properties of the fungal cell wall required to colonize different surfaces.

Spore wall

The spore wall assembles between the inner and outer forespore membranes shortly after membrane synthesis. It is composed of chitosan, glucans and mannans, and has a proteinaceous outer coat consisting mainly of Isp3 (Ohtsuka *et al.*, 2022). The spore wall consists of an inner spore wall, which is similar to the cell wall of vegetative cells, and an outer spore wall which is responsible for the ragged spore surface (Tahara *et al.*, 2020). The spore wall, along with the Isp3 layer is important for the high stress tolerance and survival of spores in harsh environmental conditions. During sporulation, the linear β-(1,3)-glucan synthesis is carried out by Bgs2 subunit of β-(1,3)-glucan synthase enzyme which localizes to the spore periphery (Martín *et al.*, 2000; Liu *et al.*). Ags1 paralogues Mok12, Mok13 and Mok14 localize to the spore envelope during sporulation and play a role in α-glucan synthesis (García *et al.*, 2006). Mok14 synthesizes α-(1,4)-glucan, which reacts with iodine to give a dark

purple color (García *et al.*, 2006; De Medina-Redondo *et al.*, 2008). Chitin is the most ancestral fungal cell wall polysaccharide, composed of β-(1,4)-N-acetylglucosamine. Although chitin is not present in the cell wall of *S. pombe* vegetative cells, it is an essential component of the spore wall (Arellano *et al.*, 2000). It is synthesized by the chitin synthase enzyme, encoded by *chs1* gene, which plays an important role in maturation of the ascospore cell wall (Arellano *et al.*, 2000; Matsuo *et al.*, 2004). Chitin is deacetylated by chitin deacetylase Cda1 to form chitosan, which is needed to form a functional spore wall (Matsuo *et al.*, 2005).

Although the spore wall is essential for spore viability and survival under harsh conditions, our current understanding of the spore wall structure and organization remains largely limited.

3. Genetic screen for genes involved in sexual reproduction in fission yeast

Sexual reproduction is tightly regulated at the molecular level and involves an array of complex processes which are largely conserved across all eukaryotes. Various genetic screens have been performed to study the mechanism of sexual reproduction. However, due to the technical limitations and low efficiency of traditional screens, the genetic mechanism governing the formation of gametes through meiosis and sexual reproduction remain poorly understood.

Billmyre *et al.,* 2022 utilized a high-throughput genome-wide Transposon insertion-sequencing assay (TN-seq) in *S. pombe* to identify the genes contributing to sexual fitness. TN-seq involves generating libraries of haploid cells with a single transposon inserted at a random site in the genome and map these sites by sequencing (van Opijnen *et al.*, 2009). Insertion at an essential gene locus disrupts its function and causes cell death, significantly diminishing the insert frequency in that gene or region. Similarly, comparative analysis across different growth conditions can be performed to identify the genes essential for survival under a certain selective pressure.

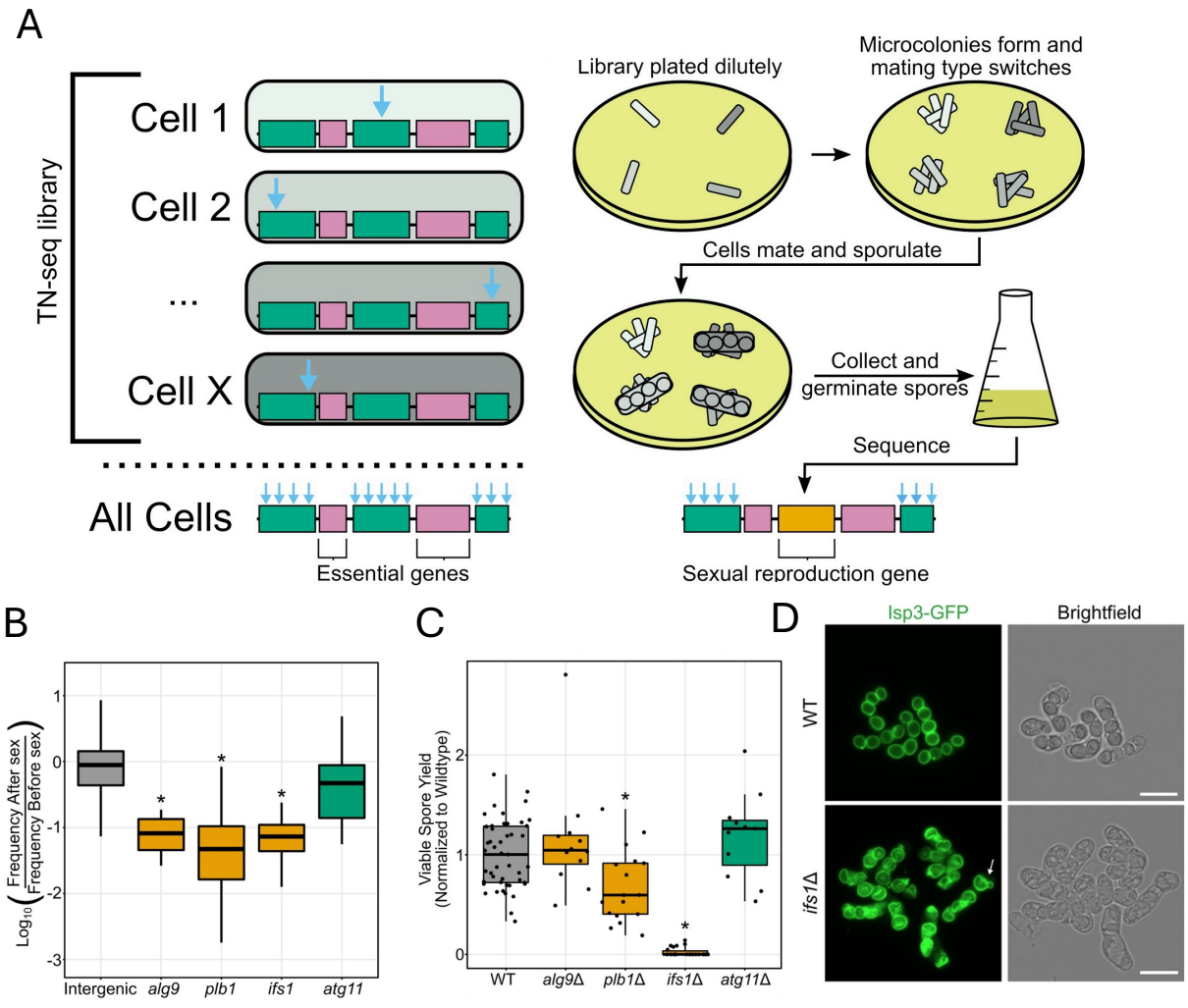

Figure 4: TN-seq to identify candidates with defects in sexual reproduction and low spore viability

(A) Schematic diagram of TN-seq to identify sexual reproduction genes. A transposon mutant library was generated by inserting transposons at random sites in the genome and insert frequency in different regions was measured via sequencing, allowing mapping of essential (pink) and non-essential (green) genes. The library was selected for ability to form viable spores by plating on sporulation media at low density allowing the cells to form microcolonies and undergo mating. The spores were collected and germinated in liquid media, and insert frequency was mapped via sequencing. Genes essential for sexual reproduction no longer have any inserts (orange). (B) Boxplot showing fold change in insert

density after sex (C) Viable spore yield assay showing for different mutants showing the number of spores obtained per cell plated, normalized to wild type average. (D) Isp3-GFP was used to visualize spore morphology in wild type and *ifs1*Δ mutants. Scale bars indicate 10 µm. Arrow indicates "snowman" spore (figure adapted Billmyre *et al.,* 2022).

For the sexual reproduction assay, a transposon-mutant library was created in a homothallic strain (h^{90}) and the cells were plated on sporulation media to induce mating and sporulation. To identify the genes essential for sex, the frequency of inserts in a gene was measured from vegetative cells (pre-sex) and in the germinated spores (post-sex). Genes with significantly lower post-sex insert frequency were candidates for playing a role in sexual reproduction. The assay identified hundreds of genes involved in sexual reproduction, including several already known genes. However, the specific roles and functions of many of the genes in the machinery of spore formation and sexual reproduction remain elusive.

Here, we addressed this gap by investigating the role of one of these genes, *ifs1* (important for sex). *ifs1*Δ mutants forms wrinkled spores with irregular morphology and very low viability. I have found that Ifs1 localizes to the nucleus during meiosis and is enriched inside the spores. I have utilized fluorescence and confocal microscopy to show that *ifs1*Δ spores form a bud-like outgrowth, giving them a "snowman"-like appearance. Electron microscopy images reveal that the spore wall of *ifs1*Δ mutants have non-uniform thickness and is weaker than that of wild type spores. During spore formation, the fragile spore wall breaks due to the high internal turgor pressure, allowing the cytoplasmic content to escape. In addition, I have also characterized the structure and biochemical activity of Ifs1 to show the highly conserved pyrophosphatase domain of Ifs1 is not essential for proper spore formation. We have also identified suppressor mutations which rescue the *ifs1*Δ mutant defects.

This study will help us gain a deeper understanding of the genetic mechanisms governing sexual reproduction in the fission yeast, providing valuable insights into the broader implications for evolutionary biology.

Results

1. *ifs1* is essential for a functional spore wall

Since *ifs1*Δ mutant forms spores with low viability, we looked at different stages of determine the steps affected by the absence of *ifs1*. We analyzed nuclear dynamics using Hht1-mRFP to look at defects during meiosis. Hht1 is a histone protein commonly used to visualize chromatin (Escorcia *et al.*) (Fig. 5A)). If *ifs1* is involved in key meiotic processes such as DNA replication or chromosome segregation, we expect to see a defect in dynamics of nuclear division.

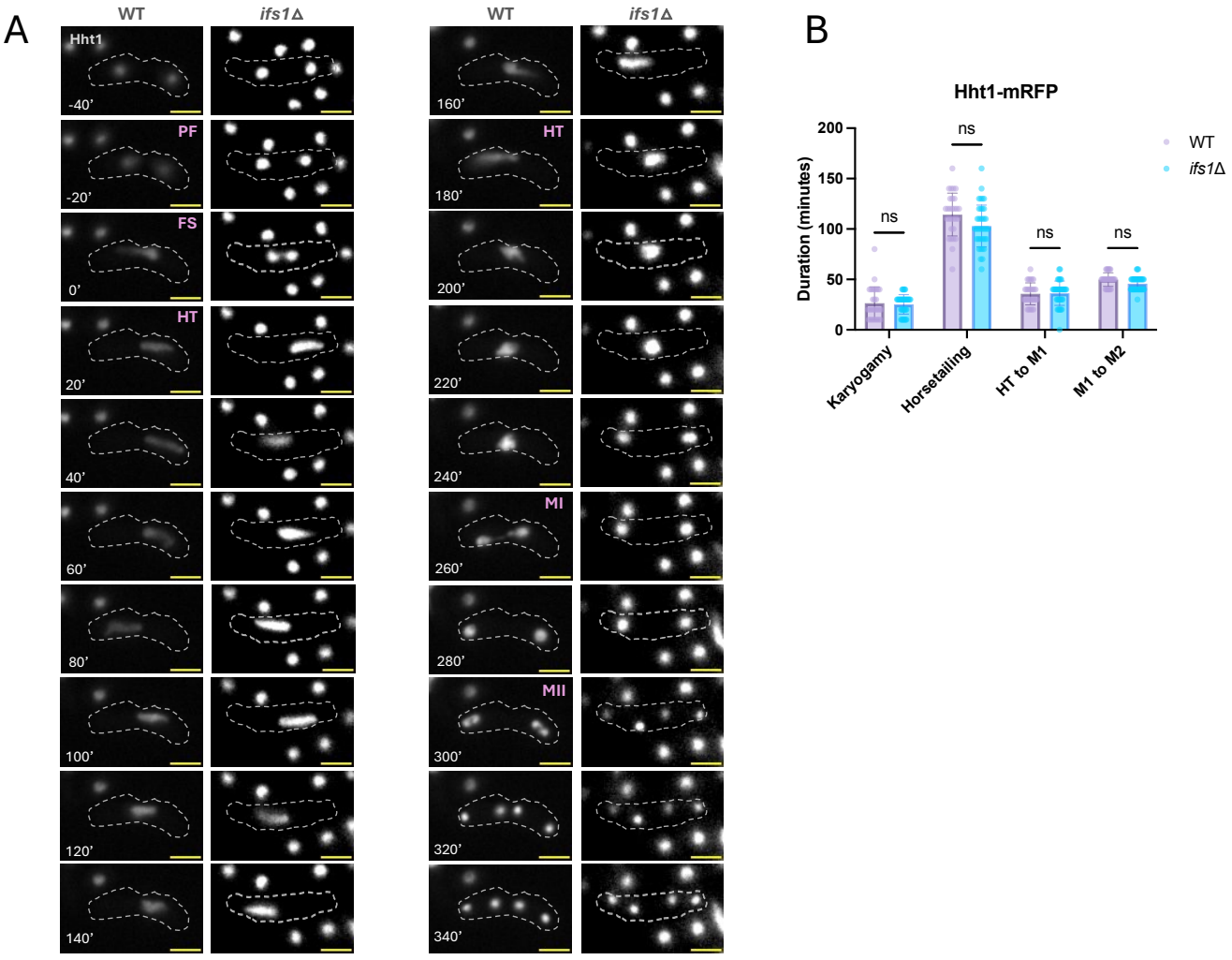

Figure 5: *ifs1*Δ mutant undergoes normal meiotic division

(A) Live-cell image of a homozygous wild type and *ifs1*Δ diploid meiotic cell visualized using Hht1-mRFP. Cells were grown on SPAS plates for 24 h at 25°C prior to imaging and images were acquired every 10 min for 24 h. The panel shows selected frames of Hht1-mRFP dynamics during meiosis with different meiotic stages such as prefusion (PF: −20 min), fusion/karyogamy (FS: 0 min), horsetailing (HT: 20-180 min), meiosis I (MI: 240-280 min), and meiosis II (MII: 300-340 min) for WT diploid. The numbers show timing in minutes and the scale bars indicate 5 µm. (B) The duration of different stages of meiosis in wild type and *ifs1*Δ mutant. Bar-graph shows the mean with standard deviation represented by error bars. n = 29 for WT and 39 for *ifs1*Δ cells. Mann-Whitney U test (ns = not significant, p>0.05)

We see that both wild type and *ifs1*Δ cells undergo mating**,** followed by nuclear fusion (10-20 min), cyclic movement of the nuclei during prophase I – horsetailing (120-150 min), and nuclear fission – meiosis I (20-40 min), and meiosis II (40-60 min) (Fig. 5A,B). There was no significant difference in the duration of each stage during meiosis and four distinct nuclei were visible at the end of meiosis II, indicating that *ifs1* is not involved in meiosis.

Next, we looked at the dynamics of spore envelope assembly in *ifs1*Δ mutant to detect defects during spore formation. Since *ifs1*Δ spores have an irregular “snowman” shape, we wanted to identify the stage at which the spores acquire this phenotype (Billmyre *et al.*, 2022). For this analysis, we looked at forespore membrane assembly and cell wall formation using Psy1-mCherry and Isp3-GFP. Psy1 is a SNARE protein, which is found in membranes of vegetative cells (Maeda *et al.*, 2009). It localizes to the newly assembling forespore membrane (Fig. 6) (Shimoda, 2004; Maeda *et al.*, 2009; Ohtsuka *et al.*, 2022). It has been used to visualize spore envelope and identify spore morphology defects during early forespore membrane formation. Isp3 coats the exterior of the spore and is used here to look at defective spore wall morphology (Fukunishi *et al.*, 2014) (Fig.6). Our still images showed

that the wild type forms round spores. However, the *ifs1*Δ spores have either round spores (red outline) or “snowman”-shaped spores (yellow outline) with a bud-like outgrowth (Fig. 6A).

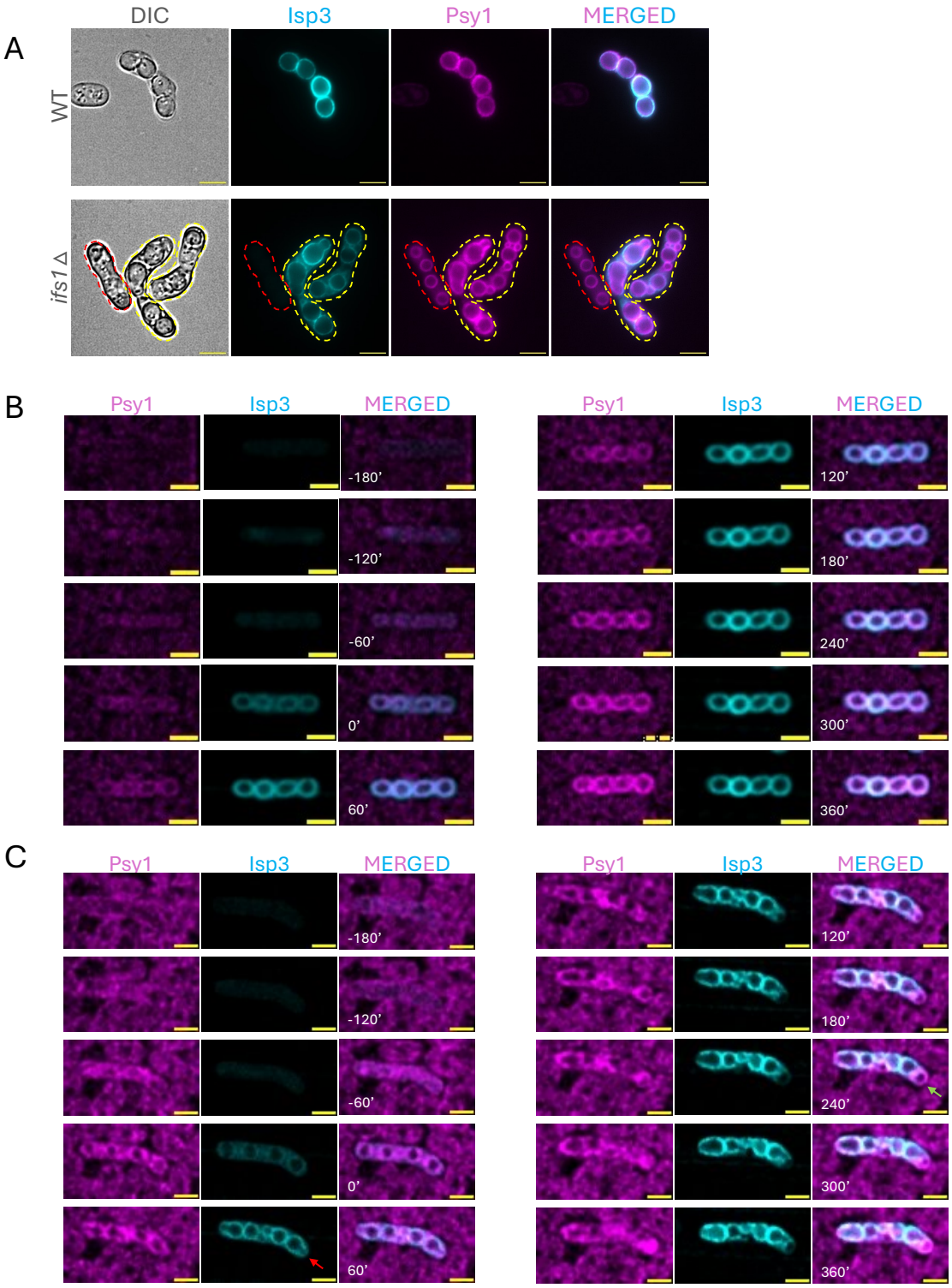

Figure 6: *ifs1*Δ mutant spores form bud-like outgrowth

(A) Still images of homozygous wild type and *ifs1*Δ ascus undergoing spore formation, visualized using Isp3-GFP (cyan) and Psy1-mCherry (magenta). Red dotted line highlights young ascus with round spores and yellow dotted lines highlight asci with mature spores showing "snowman" shape. Scale bars indicate 5 µm. (B,C) Live-cell image of a homozygous (B) wild type and (C) *ifs1*Δ ascus undergoing spore formation, visualized using Isp3-GFP (cyan) and Psy1-mCherry (magenta). Selected frames from live cell imaging are shown, and images were acquired every 10 min for 24 h. (C) Red arrow (60 min) indicates the "snowman" spore. Green arrow (240 min) indicates breaking of spore wall and plasma membrane (magenta) leaking out. The numbers show timing (min and the scale bars indicate 5 µm.

The *ifs1*Δ spores which had circular shape had very faint or no Isp3-GFP signal (Fig. 6A), suggesting that the *ifs1* defective phenotype appears after spore wall synthesis has begun since Isp3 layer forms only after spore wall has formed (Fukunishi *et al.*, 2014). We performed live cell imaging and found that initially both wild type and *ifs1*Δ appear identical and undergo proper forespore membrane closure, producing normal spherical shaped spores (Fig. 6B,C). However, after the spore wall formation begins, and Isp3 deposits outside the spore wall, a bud-like outgrowth emerges from the spore, giving it a "snowman" like appearance, marked by red arrow (Fig. 6C). This outgrowth continues to enlarge till the spore wall ruptures and the cytoplasmic material leaks out, marked by green arrow (Fig. 6C). This suggests an important role of *ifs1* in spore wall formation.

To study the defects in spore wall morphology, we utilized Scanning Electron Microscopy (SEM). SEM enabled us to study the structural and surface features of the spore, which might be contributing to low *ifs1*Δ spore viability. As previously reported, wild type spores have a sphere-like shape with outward protrusions on the surface, which is a characteristic of the outer spore wall (Nakamura *et al.*, 2004) (Fig. 7A). Whereas *ifs1*Δ spores have a small bud

on the spore (Fig. 7A(i)) and several spores have a ruptured cell wall with a bud-like outgrowth enclosed by plasma membrane emerging from the ruptured wall (Fig. 7A(ii)). Meanwhile, other spores have a collapsed cell wall with huge depressions on the surface (Fig. 7A(iii)).

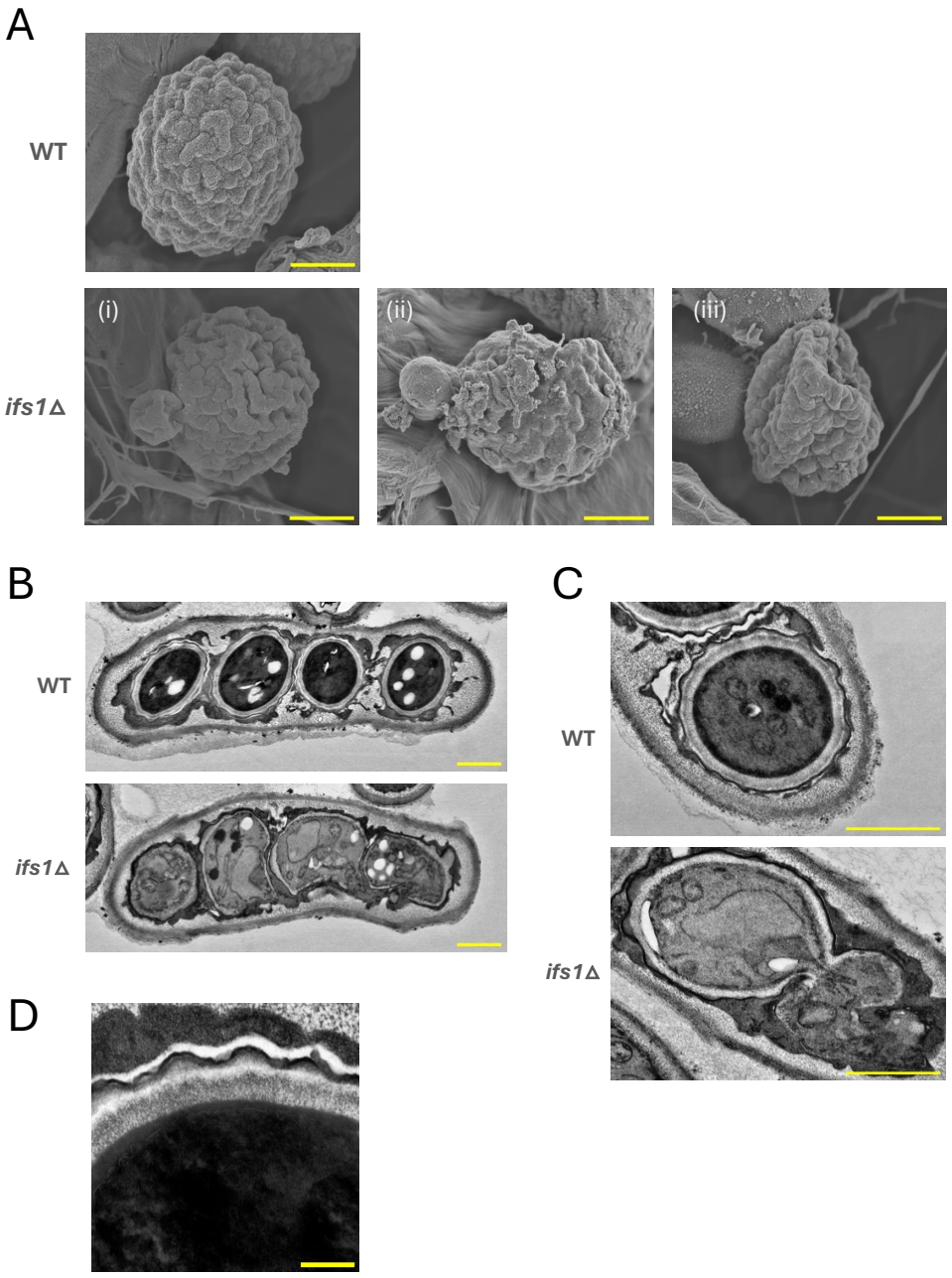

Figure 7: *ifs1*Δ mutant spores have an abnormal spore wall

(A) Scanning electron microscopy (SEM) images of wild type and *ifs1*Δ spores. Different types of phenotypes observed in *ifs1*Δ mutant spores - (i) "snowman" shaped spore with intact

spore wall, (ii) “snowman” shaped spore with broken spore wall and visible plasma membrane, and (iii) ruptured spore with a depressed surface. Scale bars indicate 1 µm. (B) Scanning transmission electron microscopy (STEM) images of wild type and *ifs1*Δ ascus carrying four spores each. Scale bars indicate 1 µm. (C) Enlarged STEM images of wild type and *ifs1*Δ spores. Scale bars indicate 1 µm. (D) Zoomed in STEM image of wild type spore showing three-layered spore wall with a dark Isp3 outer coat. Scale bars indicate 200 nm.

We also conducted scanning transmission electron microscopy (STEM) to look at the organization of the spore wall and defects in *ifs1*Δ spore wall. We saw that the wild type spores have a three-layered spore wall – inner electron-dense layer, a thin middle electron-light band and an electron-dense outer layer, which is responsible for the ridged outer surface, covered by a dark Isp3 protein coat (Fig. 7D). However, *ifs1*Δ spores have an irregular spore wall of non-uniform thickness (Fig. 7B,C). The three-layered organization of the spore wall is not observed in *ifs1*Δ spores. Instead, we see an electron-dense outer layer with several nubs and an irregular electron-light inner layer. The spore wall appears to be broken in some spores, with the content of the spore leaking out (Fig. 7C). This shows that the spore wall in *ifs1*Δ has structural defects and is weaker than that of wild type spores.

To further elucidate the role of *ifs1* in spore wall formation, we studied the composition of spore wall in *ifs1*Δ mutant. Previous studies have performed Fourier Transform Infrared (FTIR) spectroscopy to classify the components present in cell wall of *S. cerevisiae* (Galichet *et al.*, 2001). FTIR spectroscopy is a powerful analytical technique used to identify the chemical compounds present in a given sample (Griffiths, 1983; Kümmerle *et al.*, 1998). All molecules absorb infrared light of specific frequency corresponding the vibrational frequency of the chemical bonds, giving a characteristic spectrum (Griffiths, 1983). The FTIR spectrum of an unknown sample is compared to a reference spectrum to study the chemical composition of the sample.

We performed Attenuated Total Reflection-Fourier Transform Infrared (ATR-FTIR) spectroscopy study the nature of spore wall in *ifs1*Δ mutants and classify the spore wall components affected in the mutants. ATR-FTIR is a non-destructive technique which enables chemical analysis without extensive sample preparation (Kassem *et al.*, 2023). We observed many notable peaks in the spectra corresponding to different spore wall as well as other cellular components such as β-glucans (945-1180 cm^{-1}), chitin (3100 cm^{-1}), CH_2/CH_3 (2925 and 2852 cm^{-1}), thiocyanate (2159 cm^{-1}), lipids (represented by C=O at 1743 cm^{-1}), proteins (Amide I at 1643 cm^{-1} and a general protein peak at 1643 cm^{-1}), and collagen (1240 cm^{-1}) (Fig. 8A,B) (JMichell and Sourfield, 1970; Galichet *et al.*, 2001).

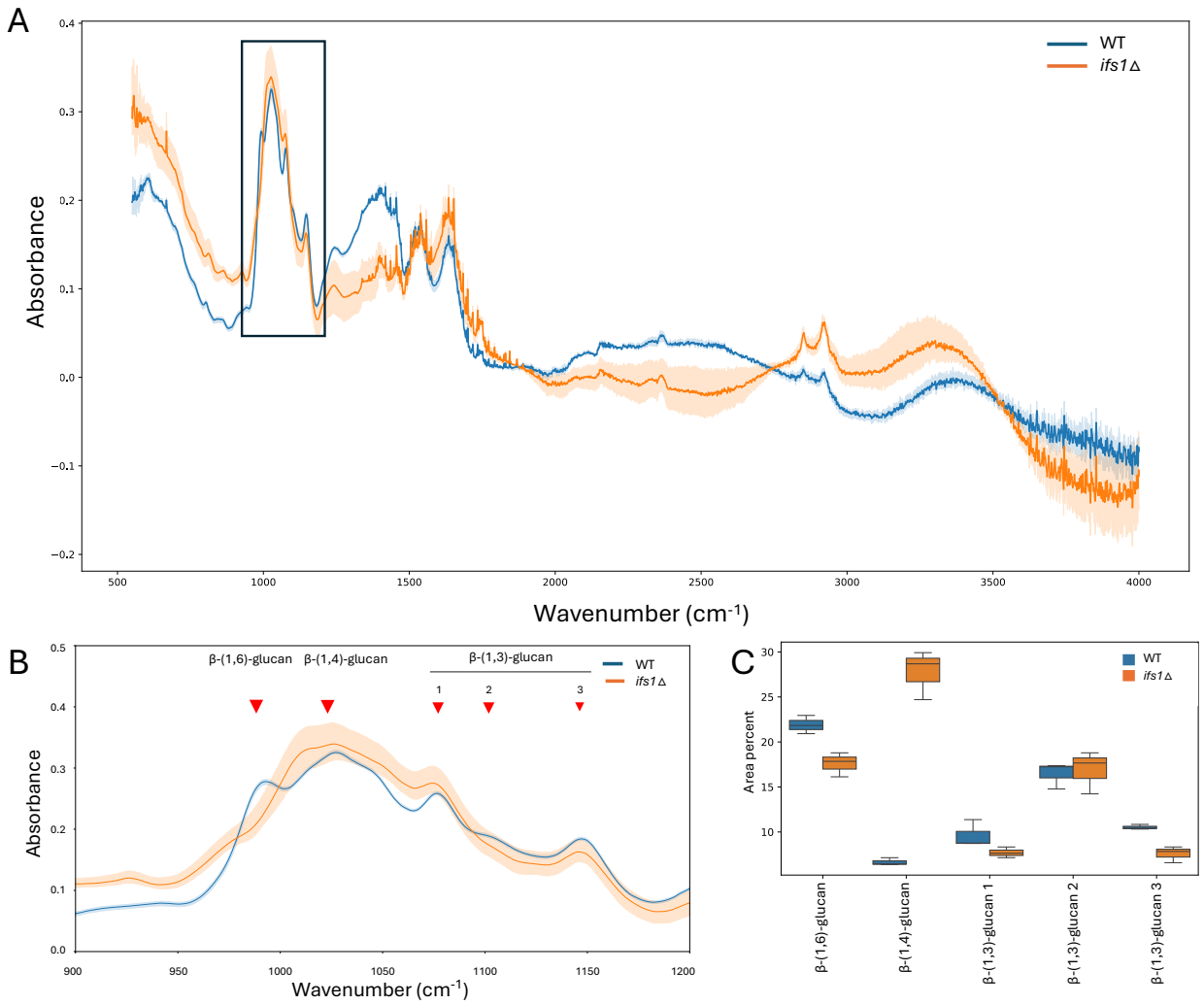

Figure 8: *ifs1* is involved in β-glucan assembly in the spore wall

(A) FTIR spectra of wild type and *ifs1*Δ mutant spores with Y-axis representing the absorbance (arbitrary units) and X-axis representing the wavenumber (cm^{-1}). n=3 for each strain. Box highlights broad β-glucan peak. (B) Zoomed in FTIR spectra showing different β-glucan peaks. (C) Comparison of percentage area contribution of individual β-glucan species to the total area between wild type and *ifs1*Δ. Box and whisker plot, with the box showing the mean percent area, and the first and third quartile. Whiskers extend from the minimum to maximum value. n = 3 biological replicates for each strain

Although the positions of peaks were similar in wild type and mutant spectra, the corresponding absorbance was significantly different for majority of the peaks (Fig. 8A,B). To examine this further, we focused on the several peaks visible in the broad β-glucan peak. We assigned β-(1,6)-glucan to 993 cm^{-1}, β-(1,4)-glucan to 1025 cm^{-1}, and β-(1,3)-glucan to peaks at 1077 cm^{-1}, 1103 cm-1, and 1140 cm^{-1}(Fig. 8B) (Galichet *et al.*, 2001). We quantified the amount of each β-glucan species by fitting multiple gaussians in the broad β-glucan peak (elaborated in Methods). Then, we compared the contribution of each β-glucan species by quantifying the area percentage of each peak to the total β-glucan peak area (Fig. 8C). We found a considerable change in the contribution of each species indicating that *ifs1* might be involved in β-glucan synthesis or organization.

2. Biochemical characterization of Ifs1

To understand the mechanistic role of Ifs1 protein in spore wall assembly, we wanted to determine if the predicted enzymatic activity of Ifs1 required for forming viable spore. AlphaFold predicted the structure of Ifs1 protein (Fig. 9B) with high confidence and a putative dTTP/UTP pyrophosphatase activity, based on structural similarity. We did PSI-BLAST to look for Ifs1 orthologs in other species and found that Ifs1 shares 30-50% sequence identity with a Maf-like protein family (Fig. 9A).

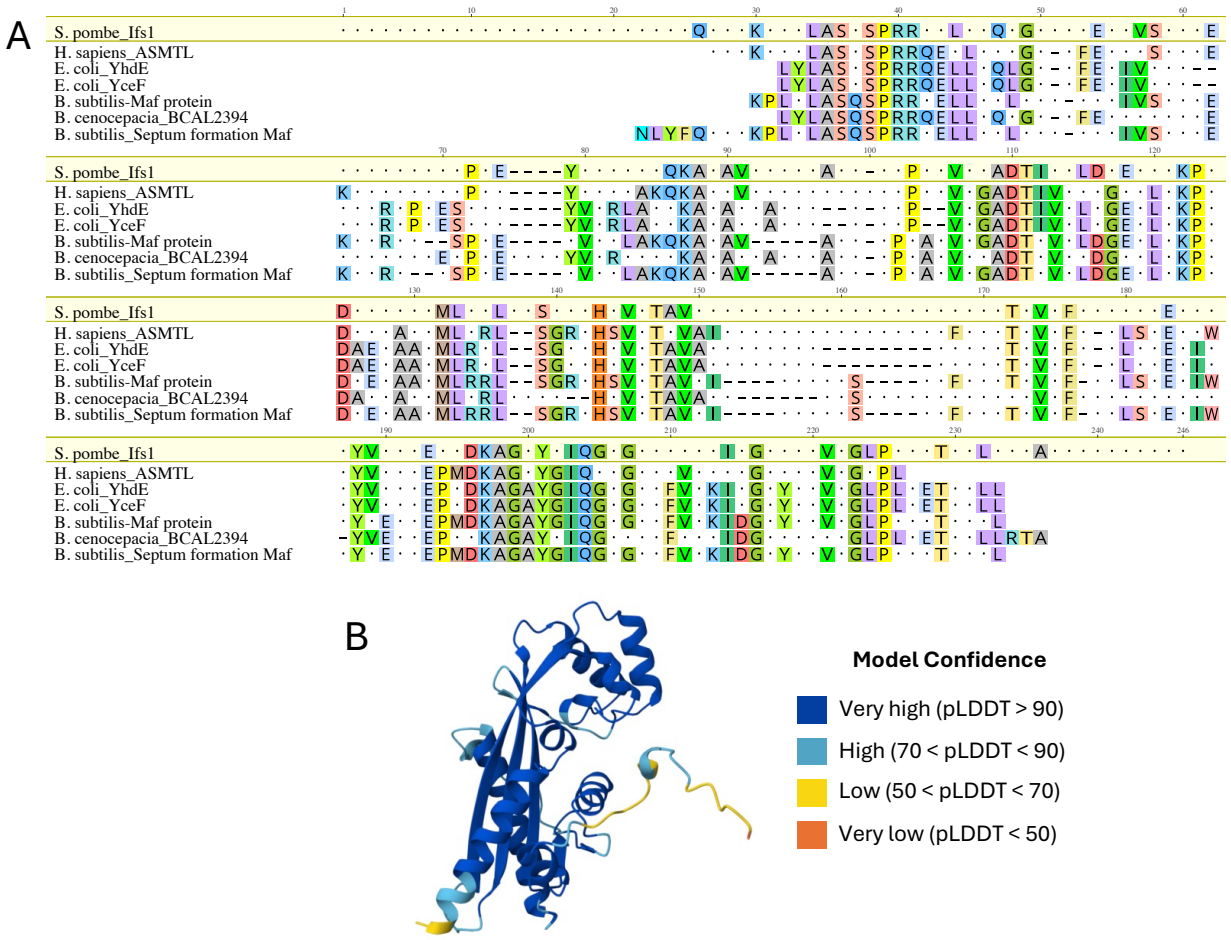

Figure 9: Ifs1 shares a conserved pyrophosphatase domain with Maf-like proteins

(A) Structure based sequence alignment of Ifs1 with Maf-like proteins orthologs from H. sapiens, E. coli, B. subtilis and B. cenocepacia. Conserved residues are represented with their respective one letter code, dots represent non-conserved residues and gaps inserted

in the alignment are indicated by hyphens. Each amino acid is highlighted by a distinct color. (B) Ifs1 protein structure predicted by AlphaFold. The chains are color-coded based on the per-residue model confidence score (pLDDT) between 0 and 100.

Although the role of Maf proteins is not well studied, their structural and biochemical properties have been characterized in six different species (Tchigvintsev *et al.*, 2013). Maf proteins share a conserved pyrophosphatase domain and have a nucleotide pyrophosphatase activity. Previous work has also identified the amino acid residues essential for the nucleotide pyrophosphatase activity, conserved across all species, and studied the enzymatic activity of proteins with a single-site mutation.

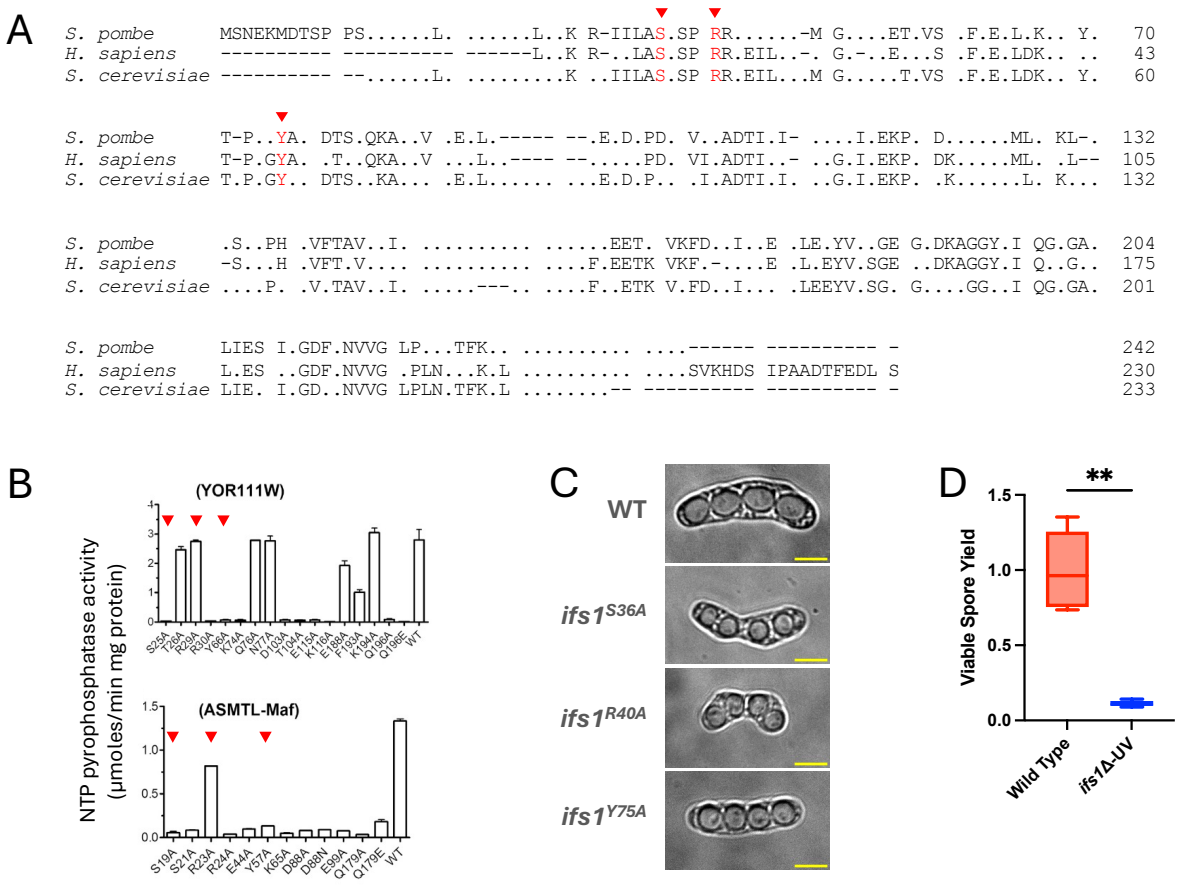

Figure 10: Site directed mutagenesis of Ifs1 in the conserved pyrophosphatase domain

(A) Structure based sequence alignment of Ifs1 with Maf-like proteins orthologs from *H. sapiens* (ASMTL-Maf) and *S. cerevisiae* (YOR111W). Conserved residues are represented with their respective one letter code, dots represent non-conserved residues and gaps inserted in the alignment are indicated by hyphens. Residues highlighted in red were replaced by alanine to construct mutant Ifs1 protein with single-site modifications. (B) Nucleotide pyrophosphatase activity of purified mutant Maf proteins measured in Tchigvintsev *et al*., 2013. The assay was conducted with 0.3 mM UTP, 2 mM Co^{2+} in YOR111W (*S. cerevisiae*) and 5 mM Co^{2+} in ASMTL-Maf (*H. sapiens*) and 0.03–0.5 mg of protein. Bar graph represents mean ± SD from at least two independent replicates (figure adapted from Tchigvintsev *et al*., 2013). (C) Still images of wild type, *ifs1*^{S36A}, *ifs1*^{R40A} and *ifs1*^{Y75A} mutant ascus showing four spores. (D) Viable spore yield assay of wild type and UV treated *ifs1*Δ strains on SPAS plate. Y-axis represents viable spore yield i.e., the number of spores formed per yeast cell plated, normalized to wild type average. n = 6 for each strain. Box and whisker plot, with the box showing the normalized mean value, and the first and third quartile. Whiskers extend from the minimum to maximum value.

We wanted to determine whether Ifs1 has a similar activity essential for its role in sporulation. For this, we generated three mutants with a single residue replaced with Ala (S36A, R40A and Y75A) and looked at the spore morphology in these mutants. The mutants were generated in an h^{90} haploid strain, with a wild type background, at the endogenous locus (elaborated in Methods). The transformed cells were self-crossed to obtain a homozygous diploid to study the sporulation associated defects. We observed that these mutant proteins with reduced pyrophosphatase activity form round spores with normal morphology (Fig. 10C), suggesting that Ifs1 doesn't require the pyrophosphatase activity for spore formation.

We also looked for mutations which suppress the *ifs1*Δ phenotype by performing random UV-mutagenesis. We irradiated vegetative cells with UV light to get 40-50% lethality, in order

to generate mutations at various regions in the genome. The mutations which rescued the *ifs1*Δ defects were selected based on their efficiency to form viable spores by inducing the UV irradiated cells to undergo successive cycles of mating and spore formation. We saw that the spore viability of the irradiated spores went up to 11% (Fig. 10D) compared to almost 0% in *ifs1*Δ mutant (Fig. 11B), indicating presence of a mutation which suppresses the defective phenotypes found in *ifs1*Δ mutant.

Earlier studies reported that *ifs1* transcript levels are enriched under phosphate starvation (Garg *et al.*, 2023). We conducted spot dilution assay on media with different phosphate concentrations to see whether *ifs1*Δ has growth defects under phosphate starvation. We observed that wild type cells grew slower on phosphate deficit media and enter a quiescent state. However, both wild type and *ifs1*Δ cells had similar growth rates, even on phosphate deficit media, indicating that *ifs1* is not required for wild-type growth under phosphate starvation (Fig. 11A). Furthermore, sporulation on media with higher phosphate levels did not rescue *ifs1*Δ spore defects and the viable spore yield was similar to that on normal media (Fig. 11B).

E. coli Maf protein YhdE has been reported to have pyrophosphatase activity associated with inhibition of cell division under various physiological conditions such as osmotic stress (Jin *et al.*, 2015). We looked at the growth curve of *ifs1*Δ cells in different NaCl concentration to determine its role in osmotic stress. However, we did not see any significant difference between the wild type and mutant growth rates (Fig. 11C). In addition, we did not see any difference between the wild type and *ifs1*Δ growth in spot dilution assay conducted at three different temperatures – 25°C, 32°C and 37°C (Fig. 11D).

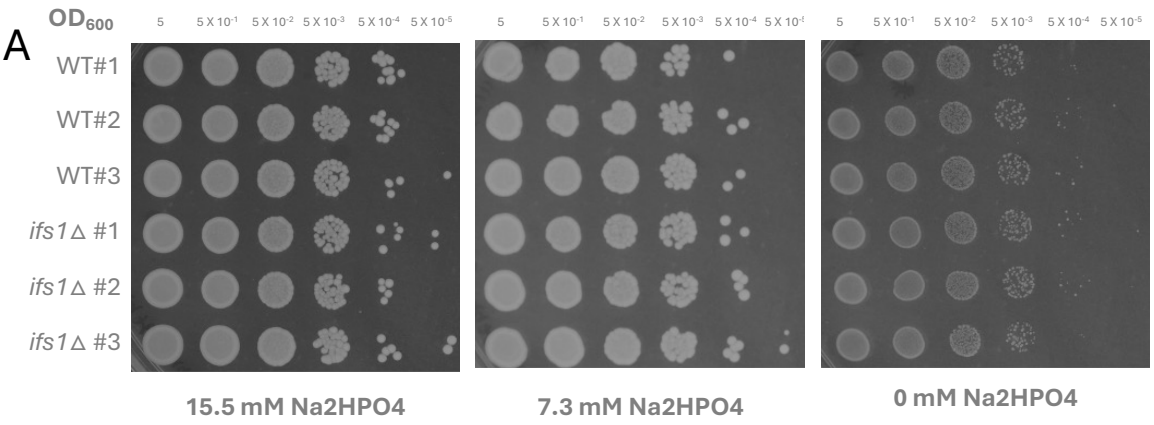
A
OD600
5
5 X 10-1
5 X 10-2
5 X 10-3
5 X 10-4
5 X 10-5
WT#1
WT#2
WT#3
ifs1Δ #1
ifs1Δ #2
ifs1Δ #3
15.5 mM Na2HPO4
7.3 mM Na2HPO4
0 mM Na2HPO4

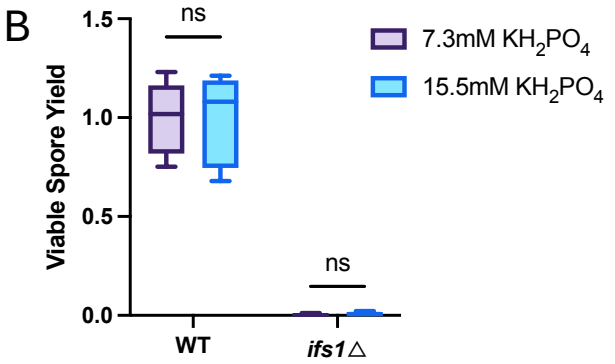
B
ns
7.3mM KH2PO4
15.5mM KH2PO4
Viable Spore Yield
1.5
1.0
0.5
0.0
ns
WT
ifs1Δ

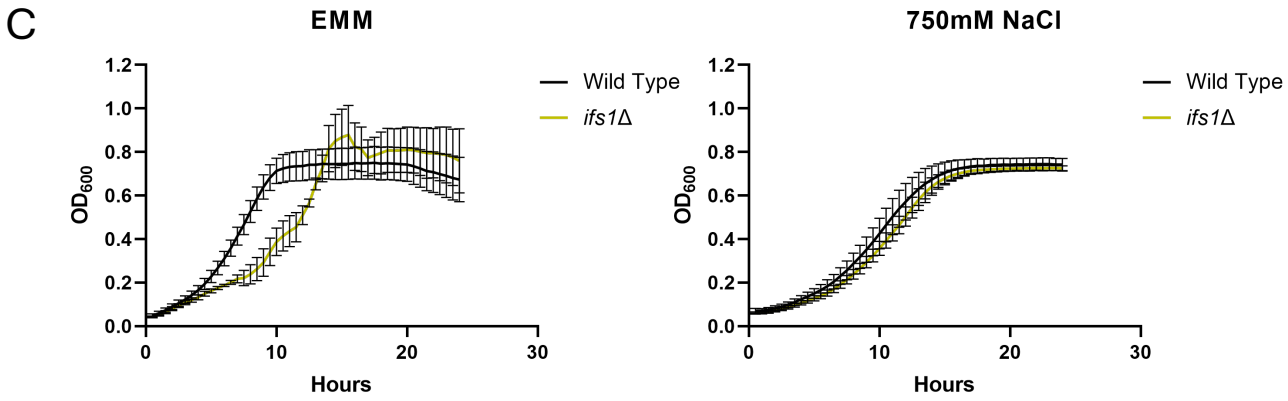
C
EMM
750mM NaCl
Wild Type
ifs1Δ
OD600
1.2
1.0
0.8
0.6
0.4
0.2
0.0
0
10
20
30
Hours

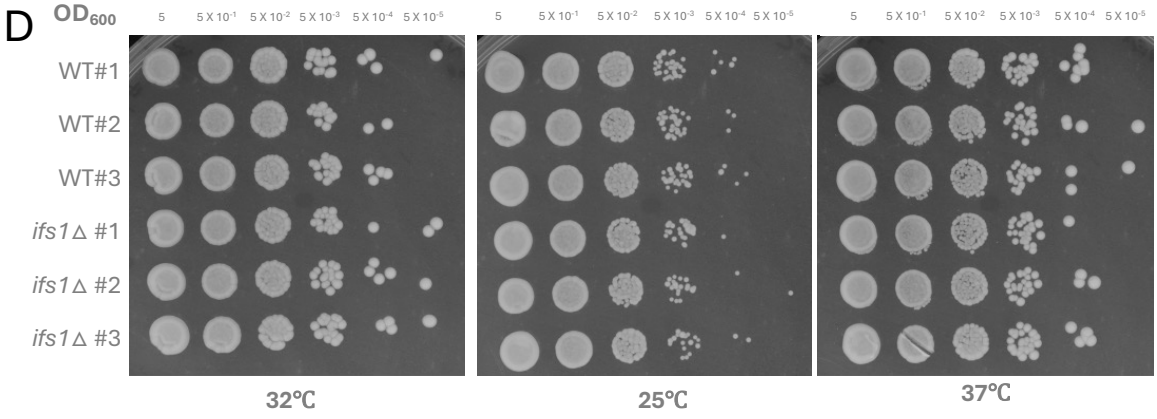
D
OD600
5
5 X 10-1
5 X 10-2
5 X 10-3
5 X 10-4
5 X 10-5
WT#1
WT#2
WT#3
ifs1Δ #1
ifs1Δ #2
ifs1Δ #3
32℃
25℃
37℃

Figure 11: *ifs1* is not important for growth under stress conditions

Spot dilution assay of wild type and ifs1Δ strains on (A) EMM plates with different phosphate concentrations or (D) YEA plates at different temperatures. A serial dilution starting from the first spot of OD_{600} = 5 culture with a successive 10-fold dilution with the final spot being $1/10^{5th}$ of the first. The plates were incubated for 3 days at (A) 32°C or (D) 25°C, 32°C and 37°C. (B) Viable spore yield assay of wild type and *ifs1*Δ strains on SPAS plate with 7.3mM KH_2PO_4 and 15.5mM KH_2PO_4. Y-axis represents viable spore yield i.e., the number of spores formed per yeast cell plated, normalized to wild type average. n = 6 for each strain on both phosphate concentrations . Box and whisker plot, with the box showing the normalized mean value, and the first and third quartile. Whiskers extend from the minimum to maximum value. Mann-Whitney U test (ns = not significant, p>0.05). (C) Growth curves of wild type and ifs1Δ vegetative cells, growing in EMM with different salt concentrations. The cells were grown at 25°C in EMM or EMM with 750mM NaCl and OD_{600}c was measured every 30 min for 24 h. n = 3 for each strain. Error bars represent standard deviation from the mean value.

3. Spatiotemporal expression of *ifs1* during meiosis

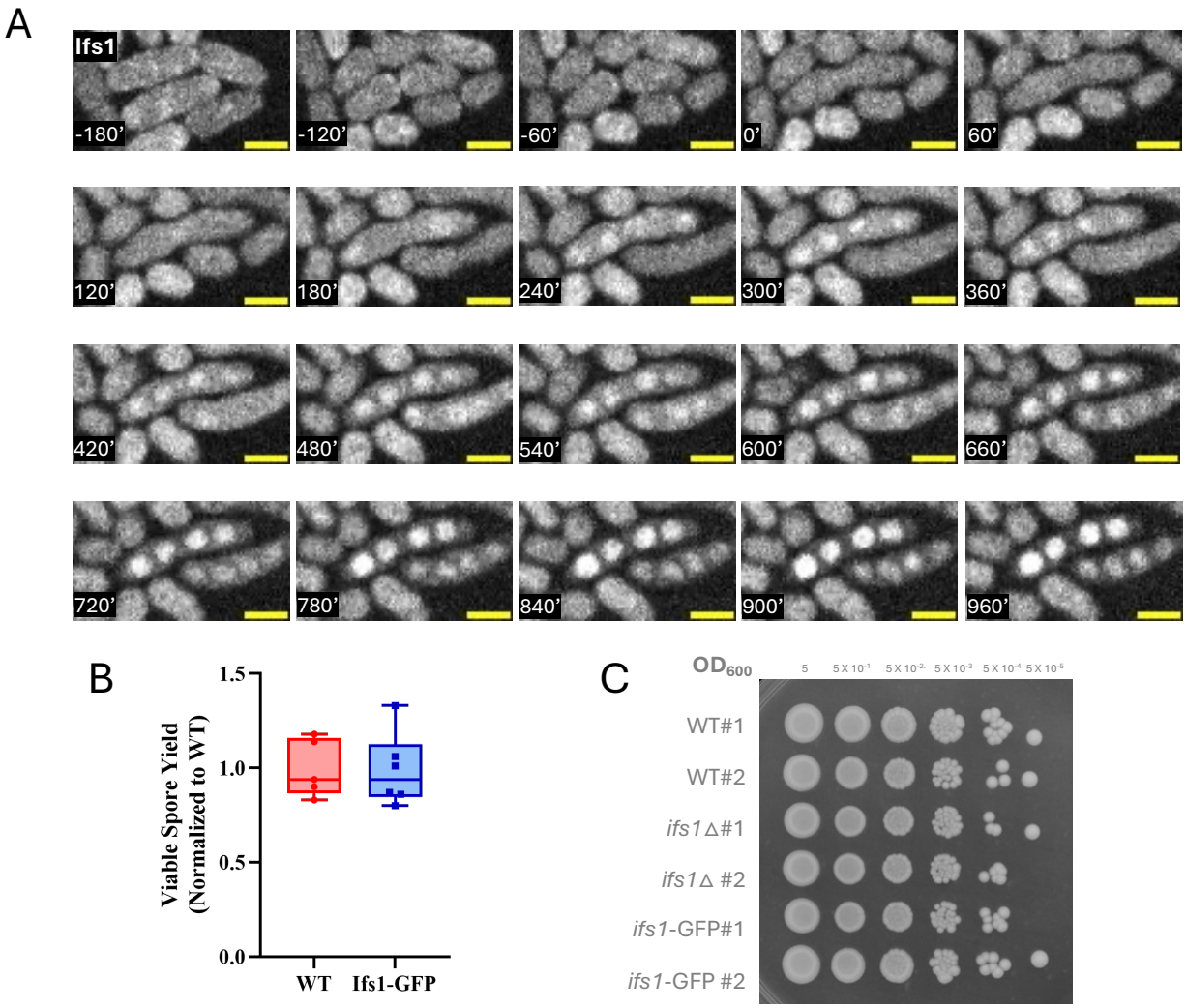

Figure 12: Ifs1 signal is enriched in the spores

(A) Live-cell image of a homozygous wild type diploid undergoing meiosis and spore formation, visualized using Ifs1-GFP (green). Selected frames from live cell imaging are shown, and images were acquired every 10 min for 24 h. The numbers represent timing (min) and t = 0' represents karyogamy. The scale bars indicate 5 µm. (B) Viable spore yield assay of wild type and Ifs1-GFP strains on SPAS plate. Y-axis represents viable spore yield i.e., the number of spores formed per yeast cell plated, normalized to wild type average. n = 6 for each strain. Box and whisker plot, with the box showing the normalized mean value, and the first and third quartile. Whiskers extend from the minimum to maximum value. (C) Spot

dilution assay of wild type, *ifs1*Δ and *ifs1-GFP* strains on YEA plates. A serial dilution starting from the first spot of OD_{600} = 5 culture with a successive 10-fold dilution with the final spot being $1/10^{5th}$ of the first. The plates were incubated for 3 days at 32°C.

Finally, we examined the expression pattern of *ifs1* through meiosis to determine the cellular process which might be associated with *ifs1*. We tracked the localization and expression of *ifs1* using a C-terminal GFP tag through meiosis and spore formation. Ifs1-GFP was expressed at the endogenous locus using the endogenous promoter, ensuring normal regulation and expression pattern. We saw that *ifs1* is constitutively expressed at low levels in vegetative cells. Most of the signal is cytoplasmic with faint nuclear localization in some cells. Following meiosis I, *ifs1* signal increases with a slight enrichment in the two nuclei. When the mature spores have formed, most of the *ifs1* signal is enriched in the spores and a very low intensity signal is seen in the ascus (Fig. 12A). Moreover, we didn't observe any mitotic growth or spore viability defects in the Ifs1-GFP strain (Fig. 12B,C).

Discussion

Sexual reproduction is a complex biological process crucial for survival of a species and evolution of life. Here, we have utilized fission yeast *Schizosaccharomyces pombe* to understand the underlying molecular mechanism of sexual reproduction. I have studied the role of a novel gene *ifs1* during sexual reproduction in fission yeast. *ifs1*Δ mutant forms spores with low viability and an irregular morphology. We have looked at different stages of sporulation, including mating, meiosis, and spore envelope formation. We have shown that Ifs1 has a vague nuclear localization during meiosis and is enriched in the spores. It is involved in spore wall formation and the spore wall of *ifs1*Δ mutant is weaker than that of WT and has non-uniform thickness. The mutant spores develop a bud-like outgrowth on the surface following spore wall formation. This phenotype is likely due to the weak cell wall which might not be able to tolerate the large internal turgor pressure of the spores, forcing the spore to expand and form a bubble-like structure, which continues to grow until the spore wall ruptures, allowing the cytoplasmic material to escape.

We have looked at the wall architecture using scanning transmission electron microscopy to study the structure of spore wall and identify defects associated with *ifs1*Δ. Earlier studies have reported the spore wall as a bilayer structure with an electron-dese outer layer and an electron-light inner layer (Tahara *et al.*, 2020). However, our images show that the spore wall is composed of three layers – an outer electron-dense layer responsible for the ridged surface, a thick, electron-dense inner band and a thin electron-light ring in the middle. We see that young developing spores only have two layers as has been shown in previous studies (Fig. 13). As the spore matures, an electron-dense material appears to deposit and form an electron-dense ring in the inner electron-transparent layer. Continuous deposition of this material prompts the ring to expand inwards to form a three-layered cell wall with a thick, electron-dense innermost layer (Fig. 13). Similar structures have been previously

observed, but not extensively described(Yoo *et al.*, 1973). Whereas the *ifs1*Δ *spore* wall has a non-uniform thickness and an abnormal morphology. Since spore wall is essential for maintaining the shape of the spore, the irregular shape of the *ifs1*Δ spores might be due to the non-uniform and fragile spore wall. Immunoelectron microscopy for individual spore wall components can be conducted to study their localization patterns in *ifs1*Δ mutant. We performed ATR-FTIR spectroscopy to study the nature of spore wall of *ifs1*Δ mutant spores. We see that the absorbance at many peaks in the spectra was different among wild type and *ifs1*Δ, showing that the spore wall composition is affected in *ifs1*Δ. We found that *ifs1*Δ spores show a considerable change in the levels of some of the β-glucans, which are essential for proper spore wall. It is possible that *ifs* might be involved in synthesis or assembly of β-glucans in the cell wall. However, since other components also showed a significant change in the spectra, it is possible that *ifs1* might contribute to other mechanisms in spore wall biogenesis.

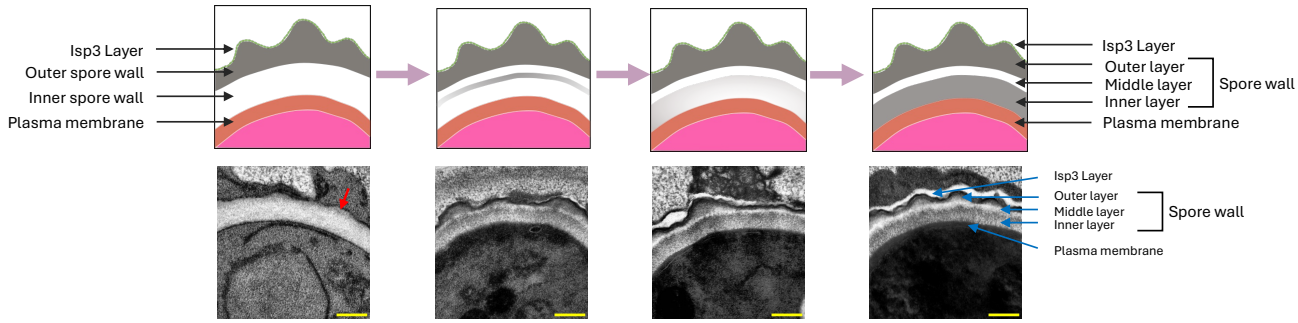

Figure 13: Spore wall maturation in fission yeast

(A) Schematic diagram representing different stages of spore wall formation in fission yeast. The spore cytoplasm is used to distinguish between young and mature spores as it becomes more electron-dense in mature spores. Young spores have a thick electron-lucent inner layer and a very thin outer spore wall, with small outward nubs (red arrow). As the spore matures, the spore plasm becomes more electron dense and an electron-dense ring forms in the inner spore wall. The outer layer shows more prominent nubs with a dark Isp3 layer forming the outer coat. The electron-dense ring expands inwards forming a three-layered cell wall

with a thick electron-dense inner layer, a thin electron-light middle band and a dark outer layer responsible for the ragged surface. Scale bars indicate 200 nm.

I also performed structural analysis of Ifs1 protein to understand the enzymatic activity of Ifs1 essential for a functional spore wall. Ifs1 has 25-45% sequence identity to Maf-like proteins, a large family of proteins conserved across bacteria, archaea and eukaryotes. However, their functions are largely unknown. Introduction of *maf* gene in *B. subtilis* has been reported to inhibit cell division and cause extensive filamentation (Butler *et al.*, 1993). *B. subtilis* Maf has been crystallized in a dUTP-bound state, and is reported to have structural similarity with nucleotide triphosphate pyrophosphatases (Minasov *et al.*, 2000). *E. coli* Maf YhdE has a pyrophosphatase activity involved in cell division inhibition (Jin *et al.*, 2015). Tchigvintsev *et al.*, 2013 characterized the biochemical activity and structure of six Maf proteins, from bacteria to eukaryotes. Maf proteins have a conserved nucleotide triphosphate pyrophosphatase activity against canonical as well as non-canonical nucleotides. To determine whether the pyrophosphatase activity of Ifs1 is required for spore formation, I engineered single-site mutation in the conserved pyrophosphatase domain at residues which have been characterized earlier in other orthologs (Tchigvintsev *et al.*, 2013). However, I didn't see any change in spore viability or morphology, suggesting that the pyrophosphatase activity of Ifs1 is not required in sporulation. It is possible that the mutant Ifs1 protein is able to carry out the required pyrophosphatase activity and future experiments will involve purification and in vitro analysis of the pyrophosphatase activity of mutant Ifs1 protein.

Spore wall of fission yeast has a multilayer organization and is composed of several distinct polysaccharides. Various genes are involved in spore wall assembly and disruption of any of these genes results in severe spore viability defects. Deletion of *bgs2* gene, involved in β-glucan synthesis in spores, results in spores with irregular morphology, which lack the inner spore wall. *bgs2*Δ diploids formed non-viable spores which lysed upon being released from

the ascus (Martín *et al.*, 2000; Liu *et al.*). *mok12,mok13 and mok14* genes, involved in α-glucan synthesis, are essential for functional spore wall. Deletion of these genes results in reduced spore viability, increased sensitivity to environmental stress and negative iodine staining (García *et al.*, 2006). In addition, various other genes have been identified to be involved in envelope formation, some of the genes which show similar "snowman"-shaped spores are listed in table 1.

Gene	Function in sporulation
meu10	Spore wall maturation, β-(1,3)-glucan localization
meu14	Spindle pole body assembly and forespore membrane extension
mug28	Forespore membrane formation and closure of leading edge
sst4	Forespore membrane extension and closure of leading edge

Table 1: Genes associated with "snowman" spore phenotype

The role of these genes was discovered in the following studies - *meu10* (Tougan *et al.*, 2002), *meu14* (Okuzaki *et al.*, 2003), *mug28* (Shigehisa *et al.*, 2010) *and sst4* (Onishi *et al.*, 2007)

*meu10*Δ spores have an uneven thickness and show abnormal β-(1,3)-glucan localization. The spore wall is much thicker than that of wild type and all the spores are non-viable (Tougan *et al.*, 2002). *meu14* is found at the leading edge of forespore membrane and is required for proper extension of the membrane (Shigehisa *et al.*, 2010). *meu14*Δ diploids fail to form spores due to defective forespore membrane assembly. EM images show that some nuclei are either enclosed by incomplete or non-homogenous wall or completely lack the spore wall (Okuzaki *et al.*, 2003). *mug28*Δ cells show a delayed disappearance of Meu14, causing aberrant forespore membrane formation and improper membrane ring closure. *mug28*Δ spores have a thicker wall and the cytoplasm of the bud, and the spore is separated by the spore wall in "snowman" spores (Shigehisa *et al.*, 2010). Sst4p works downstream of

Pik3p and is required for proper forespore membrane closure. *sst4*Δ mutants fail to close the ring and bubble-like structures emerge from the unclosed leading edge (Onishi *et al.*, 2007).

Unlike *meu14, mug28 and sst4, ifs1* is not involved in forespore membrane assembly and the *ifs1*Δ cells are able to perform proper ring closure. On the contrary, *ifs1*Δ mutants develop the "snowman"-shape after the forespore membrane has formed and the spore wall synthesis has begun. Since *meu10* is involved in spore wall assembly and absence of *meu10* leads to abnormal β-(1,3)-glucan localization, it is possible that *meu10* and *ifs1* have closely related functions. To further elucidate the mechanistic role of *ifs1* in spore wall synthesis, future experiments will involve studying the relationship of *ifs1* with these genes.

Identifying the mutations in the UV-irradiated *ifs1*Δ cells by whole-genome sequencing will allow us to assess the genetic interactions of *ifs1*. This might help us unravel the mechanistic pathway which engages the Ifs1 protein for its role in spore wall formation.

Materials and methods

1. Yeast strains and media

The *S. pombe* strains used in this study are listed in Table 3. Complete medium YE+sup (Table 2) and synthetic medium EMM (Table 2) were used for growth, and malt extract (ME) (Table 2) and SPAS (Table 2) media were used for setting up crosses and sporulation.

Media	Composition
YE+sup	0.5% yeast extract, 3% dextrose, 200 mg/L adenine, histidine, leucine, lysine, and uracil, and agar (for plates)
EMM	0.3% potassium phthalate monobasic, 0.415% $Na_2HPO_4.7H_2O$, 2% dextrose, 0.5% ammonium chloride, 250mg/L of adenine, histidine, lysine, leucine and uracil, and agar (for plates)
SPAS	1% glucose, 7.3 mM KH_2PO_4, vitamins, 45 mg/L adenine, histidine, leucine, lysine, and uracil and agar
ME	3% malt extract, 200 mg/L adenine, histidine, leucine, lysine, and uracil, and agar (for plates)

Table 2: List of all the media used with their composition

The cells were grown at 32°C and crosses were set up at 25°C. Strains were generated by crossing on sporulation media and screening for spores with desired genotypes (Smith, 2009).

Strain number	Genotype
SZY4498	h90*, leu1-32, ura4-D18 ifs1Δ::KANMX4*
SZY4975	h90 *isp3-GFP leu1<<mCherry-psy1*
SZY4976	h90, *leu1-32, ura4-D18*
SZY5082	h90 *isp3-GFP leu1<<mCherry-psy1, ifs1Δ::kanMX4*
SZY5165	h90, *hht1-mRFP:hphMX6, leu1-32, ura4-D18, his-D1*
SZY5319	h90*, ifs1-GFP-KanMX6, leu1-32, ura4-D18*
SZY6934	h90, *ifs1-GFP-KANMX, hht1-mRFP-HYGMX, leu1-32, ura4-D18*; Isolate 1
SZY6936	h90, *ifs1Δ::KANMX, hht1-mRFP-HYGMX, leu1-32, ura4-D18*; Isolate 1
SZY7139	h90, *leu1-32, ura4-D18 ifs1Δ::ura4*
SZY7265	h90, *leu1-32, ura4-D18 ifs1-S36A*
SZY7267	h90*, leu1-32, ura4-D18 ifs1-R40A*
SZY7269	h90*, leu1-32, ura4-D18 ifs1-Y75A*

Table 3: List of all the strains used and their genotypes

2. Site directed mutagenesis

Oligos containing homology regions to the 5' and 3' UTR of *ifs1* (5016, 5017) were used to amplify the *ura4* gene using the pSZB1498 plasmid as a template, generating a *ura4* construct with ends homologous to the *ifs1* UTR. The *ifs1Δ::KANMX4* strain (SEZ4498) was then transformed with this construct to obtain *ifs1Δ::ura4* (SEZ7139), which subsequently served as the background for generating single-site mutants.. *ifs1* gene was amplified using two different sets of oligos, listed in table 4, to create two overlapping fragments carrying the desired mutation. The two amplified fragments carrying the mutation were stitched together with a PCR using oligos flanking the *ifs1* 3' and 5' UTR (5069, 5070). The resulting stitched PCR product, comprising the complete *ifs1* gene with the desired mutation, was transformed into the *ifs1Δ::ura4* strain to generate the desired mutants. 5-FOA plates were used to select for transformants, which were additionally confirmed by PCR and sanger

sequencing. The transformations were carried out following the standard lithium acetate transformation protocol (Gietz *et al.*, 1995). All the oligos and plasmids used are listed in table 4 and 5, respectively.

Oligo Number	**Oligo name**	**Sequence**
5016	*ifs1*Δ::*ura4* Deletion for	CAAAAAACAACTTTGAGTTAAATTTGTTGAGTTCAAATCATT TTTCAAAGTTTACTTCTTATGGATGCTAGAGTATTTCA
5017	*ifs1*Δ::*ura4* Deletion rev	TAGTTAATATGTAAAGGAATTTAAACAAAAACATTGAAGTGT ATGAGGCAAAGATGAAGGTTAATGCTGAGAAAGTCTTT
5018	*ifs1* 5' UTR seq for	CTCTTTCAAAGCTTCTCTTC
5019	*ura4* internal seq rev	GAAATACCGTCAAGCTACAA
5020	*ura4* internal seq for	TTTAACATCCAAGCCGATAC
5021	*ifs1* 3' UTR seq rev	GGTTCTTTCATGACTCTAAG
5022	*ifs1* internal seq for	CTATGGAAGTGCCTATTCAT
5061	Ifs1_S36A_FP HiFi	TTTTGGCTGCAGGATCCCCT
5062	Ifs1_S36A_RP HiFi	AGGGGATCCTGCAGCCAAAA
5063	Ifs1_R40A_FP HiFi	CCCTGCCAGAAAGCAGTTAT
5064	Ifs1_R40A_RP HiFi	ATAACTGCTTTCTGGCAGGG
5065	Ifs1_Y75A_FP HiFi	TTGGGAAGCTGCTGCTGACA
5066	Ifs1_Y75A_RP HiFi	TGTCAGCAGCAGCTTCCCAA
5067	Ifs1_R41A_FP HiFi	CTCGCGCAAAGCAGTTATTT
5068	Ifs1_R41A_RP HiFi	AAATAACTGCTTTGCGCGAG
5069	Ifs1_5'UTR_FP HiFi	CACATTAAAATCGGTCCTGA
5070	Ifs1_3'UTR_RP HiFi	TTGCTGGTTCTGTAAATACG

Table 4: List of all the oligos used with their names and sequence

Plasmid Number	Yeast marker	Description
pSZB1498	*ura4*	pSZB1377 (dFnCas12 entry vector) loaded with sgRNA array targeting SPAC11D3.14c transcription by Golden gate cloning. Confirmed by sequencing (only gRNA), isolate 2 oligos 3549+3550

Table 5: List of all the plasmids used their respective yeast markers and their description

3. Viable spore yield

3 colonies of each strain were inoculated in YEL and grown overnight at 32°C. Two patches were made on SPAS plate from 50 µL of the saturated culture. At the same time, two $1/10^{5th}$ dilutions were prepared from each culture, and 100 µL of the dilution was plated on YEA_{SUP} plates to get the number of cells in 1 mL giving an estimate for the number of cells in each patch. All the plates were incubated at 25°C for 6 days. After 6 days, the entire patches were scraped off the plates and resuspended in sterile water. 6 µL of gluculase mix was added to each tube and incubated overnight at 32°C to digest the ascus and isolate the spores. Then, $1/10^{5th}$ dilution of each spore mix was prepared, and 100µL of the dilution was plated on YEA_{SUP} plates with the number of colonies representing number of viable spores obtained. Viable spore yield was calculated by dividing the number of colonies in the post-meiotic plate by the number of cells originally plated. The viable spore yield (VSY) for each experiment was normalized to the average VSY for WT strain used in that experiment. GraphPad Prism (https://www.graphpad.com/) was used to plot the box and whisker plot and conduct Mann-Whitney U test, with the data from 6 biological replicates for each strain.

4. Spot dilution assay

Overnight cultures were inoculated in YEL from a single colony and grown at 32°C. OD_{600} of the saturated cultures was measured using a spectrophotometer. The cultures were pelleted

and resuspended in YEL or sterile water to adjust the concentration and reach the final OD_{600} of 5. 10-fold serial dilutions were made using the resuspended culture to a final concentration of OD_{600} = 5 X 10^{-5}. 5 µL of each dilution was spotted on the plates and incubated at the specified temperature. Plates were imaged post 2 days, 3 days and 4 days of growth.

5. Growth curve assay

Overnight cultures were inoculated in YEL from a single colony and grown at 32°C. OD_{600} of the saturated cultures was measured using a spectrophotometer. The cultures were pelleted and resuspended in YEL or sterile water to adjust the concentration and reach the final OD_{600} of 2. A 96 well plate was used to dilute resuspended culture to OD_{600} of 0.2 in liquid EMM with different NaCl concentrations (normal EMM, 250mM, 500mM, 750mM, 1M and 1.25M). Tecan Infinite 200 pro plate reader was used to perform the assay. The cultures were incubated with shaking at 32°C for 24 hours. The cell growth was monitored by taking OD_{600} measurements of each well every 30 min. The growth curve was plotted using GraphPad Prism (https://www.graphpad.com/), with the data from 3 biological replicates at each time point.

6. Microscopy

6.1 Setting up crosses for imaging

Primary culture was inoculated in YEL from a single colony and grown at 32°C overnight. A secondary culture ,starting with OD_{600} of 0.2 was set up using the primary culture in 5mL EMM and grown at 32°C for 6-8 hours. The secondary culture was pelleted by centrifuging at 3000 rpm for 5 min and washed twice with sterile water. Finally, the pellet was resuspended in 2mL water and multiples patches were made with 10µL of suspension on MEA plates. The plate was incubated at 25°C for 24 hours. Hht1-mRFP time-lapse images were taken on MEA plate.

6.2 Timelapse imaging of meiosis and spore formation

A circular agar plug was punched out from the patch and placed inverted into a 35mm glass bottom dish containing a wet kim-wipe and sealed with vacuum grease (López Hernández *et al.*, 2021). The temperature was maintained using a stage top incubator (Oko Lab) at 25°C during image acquisition. Hht1-mRFP timelapse images of meiosis were acquired using Nikon Ti2-E widefield microscope. The images were taken every 10 minutes for 24 hours with a Plan Apochromat 60X objective (1.4 NA), with excitation for mRFP through a 550/15 nm excitation filter and collection through an ET595/40 m emission filter. Transmitted light images were also acquired.

All other timelapse images were acquired on Nikon Ti microscope coupled to a CSU W1 Spinning Disc (Yokogawa). Images were collected through a 60x Plan Apochromat objective (NA 1.4) with excitation for GFP at 488nm and for mCherry at 561nm and through an ET525/36 filter for GFP and an ET605/70, filter for mCherry onto an EMCCD camera (Andor iXon DU 897 Ultra). Transmitted light images were also acquired.
A single z position was maintained throughout the timelapse using Perfect Focus in all the experiments.

6.3 Still imaging of ascospores

Some cells were scraped off the MEA plate after 40 hours and resuspended in sterile water on glass slides for imaging. Images were taken with Zeiss Axio Observer.Z1 wide-field microscope through a 63x Plan Apochromat (1.4 NA) oil-immersion objective. mCherry was excited with a 530-585nm filter and reflected off an FT 600 dichroic filter to the objective. The emission was collected using a 615 nm filter. GFP was excited with a 440–470 nm filter and reflected off an FT 495 nm dichroic filter to the objective. The emission was collected using a 525–550 nm filter.

6.4 Scanning electron microscopy (SEM)

Spores were scraped off the SPAS plate after 3 days and fixed in 50mM fixative containing 2.5% glutaraldehyde, 2% paraformaldehyde, 1mM CaCl2, 1% sucrose buffered with 50mM Na Cacodylate with pH 7.4 at 25°C for two hours and stored in fixative overnight at 40°C. Wild type spores were treated with gluculase for 12-16 hours before fixation. Spores were run through a TOTO protocol (Jongebloed *et al.*, 1999). Briefly, spores were rinsed in 6 changes of ultrapure water incubated for 5 minutes each and this wash regime was carried out for all subsequent wash steps below. After the initial wash, spores were incubated in 1% filtered aqueous tannic acid for an hour at room temperature and washed as described above. Spores were then incubated for 1 hour at room temperature in 1% aqueous osmium tetraoxide, washed again, and then incubated for an hour at room temperature in 2% filtered aqueous thiocarbohydrizide (prepared the day prior). The spores were washed and incubated a second and final time in 1% aqueous osmium tetraoxide at room temperature. After a final water rinse series, the spores were dehydrated in the following series of ethanol with 15-minute incubations: 30,50,70,80,90 and three changes of 100%. Spores were critical point dried in a Tousimis Samdri-795 and sprinkled onto a stub with a section of kim-wipe on top. The stub was then coated with 4nm of Au/Pd using a Leica Ace 6000 sputter coater. Spores were imaged at 3kV, 50pA with an In Lens SE2 detector on a Zeiss Merlin SEM.

6.5 Scanning transmission electron microscopy (STEM)

Cells were scraped off the SPAS plate after 24 hours of growth and suspended in 1mL sterile water. They were immediately fixed with 1.5% KMnO4 on ice for 30 minutes and then rinsed with ultrapure water six times for 5 minutes at room temperature (Frankl *et al.*). The washed pellet was resuspended in 1% low-melt agarose and then cut into pieces smaller than 1mm3. These blocks were sequentially dehydrated in a

series of 30,50,70,80,90 and then 3 changes of 100% ethanol with all steps incubated for 15 minutes at room temperature. The samples were then moved into liquid Hard Plus resin with an accelerator the following series of dilutions: 25,50, and 75% resin. At this stage, the samples were moved to 100% resin and microwaved (Pelco Biowave) with 250W for 3 minutes and then incubated overnight at room temperature. The following morning the 100% resin was refreshed and microwaved with the same settings. At the end of the day, the resin was refreshed, microwaved again, and left overnight at room temperature. The next morning the samples were exchanged into a final 100% resin and microwaved a final time. Samples were embedded and polymerized at 60OC for 48 hours. Sections were cut at 80nm on a Leica Arctos ultramicrotome and put onto slot grids that were post-stained for 3 minutes with 1% Sato's Triple Lead, 4 minutes with 4% uranyl acetate in 70% methanol, and 5 minutes with 1% Sato's Triple Lead. Grids were imaged on a Zeiss Merlin SEM with a STEM detector at 30kV 700pA.

7. Image Analysis

Fiji was used to analyze and annotate the microscopy images (Schindelin *et al.*, 2012). SEM and STEM images were processed with the CLAHE function with the following parameters: 127, 256, 1.5 (Zuiderveld, 1994). Stage drift was eliminated using the "stackregj" plugin in the timelapse images. Background subtraction tool was used with 50-pixels rolling ball radius in all fluorescence images, which were also smoothened with a 1-pixel Gaussian blur.

8. ATR-FTIR Spectroscopy

3 colonies of each strain were inoculated in YEL and grown overnight at 32°C. Multiple patches were made on SPAS plate from 50 μL of the saturated culture and the plates were incubated at 25°C for 6 days. After 6 days, the entire patches were scraped off the plates and resuspended in sterile water. 6 μL of gluculase mix was added to each tube and incubated

overnight at 32°C to digest the ascus and isolate the spores. The gluculase was removed by washing the spores twice with sterile water. All the water was removed, and spores were dried completely. Spectra were acquired on an iS10 FTIR spectrometer (Thermo Scientific) equipped with an Attenuated Total Reflection (ATR) sample holder. Spectra were acquired from an average of 64 scans with 2 cm-1 resolution. Spectra were acquired by placing the spore pellet onto the ATR surface and pressing it down with the anvil. Many notable peaks were observed in the spectra. We assigned β-(1,6)-glucan to 993 cm^{-1}, β-(1,4)-glucan to 1025 cm^{-1}, and β-(1,3)-glucan to peaks at 1077 cm^{-1}, 1103 cm-1, and 1140 cm^{-1} (Galichet *et al.*, 2001). To measure the amount of each beta-glucan species, multiple gaussians were fit to the main β-glucan peak using an in-house python script. Gaussians were initialized at each wavenumber position as listed above including two peaks at 1013 cm-1 and 1047 cm-1 which are unknown. The peak height, position and standard deviation were allowed to fit via non-linear least squares. Then the peak areas for each component were calculated and the percent area of each component was reported. Three biological replicates were measured for each sample and the average percent area and standard error were calculated.

9. Random UV-mutagenesis

A large number of vegetative *ifs1*Δ cells were plated on YEA_{SUP} plates and treated with 200μJ/mm^2 of UV radiation to achieve 40-50% lethality. The treated plates were then incubated at 32°C. After 3 days, the YEA plate with a lawn of cells was replica plated onto SPAS media and the cells were allowed to mate and form spores at 25°C. After 6 days, the spores were collected in a 1.5mL tub and treated with gluculase for 14-16 h. The spores were pelleted and washed twice with sterile water and resuspended in 1mL water. A $1/10^{5th}$ dilution of spore suspension was made and 100μL was plated on YEA_{SUP} plates. This was repeated till the number of colonies obtained on YEA_{SUP} plates increased. After 4 successive cycles of mating and sporulation, a viable spore yield assay was performed using three independent colonies obtained from the YEA_{SUP} plate.

References

1. Alberts, B, Johnson, A, Lewis, J, Raff, M, Roberts, K, and Walter, P (2002). The Benefits of Sex. In: Molecular Biology of the Cell. 4th Edition, Garland Science.

2. Arellano, M, Cartagena-Lirola, H, Nasser Hajibagheri, MA, Durán, A, and Henar Valdivieso, M (2000). Proper ascospore maturation requires the *chs1*$^{+}$ chitin synthase gene in *Schizosaccharomyces pombe*. Molecular Microbiology 35, 79–89.

3. Arellano, M, Durán, A, and Pérez, P (1996). Rho 1 GTPase activates the (1–3)beta-D-glucan synthase and is involved in Schizosaccharomyces pombe morphogenesis. The EMBO Journal 15, 4584–4591.

4. Beach, DH, and Klar, AJ (1984). Rearrangements of the transposable mating-type cassettes of fission yeast. The EMBO Journal 3, 603–610.

5. Billmyre, RB, Eickbush, MT, Craig, CJ, Lange, JJ, Wood, C, Helston, RM, and Zanders, SE (2022). Genome-wide quantification of contributions to sexual fitness identifies genes required for spore viability and health in fission yeast. PLoS Genet 18, e1010462.

6. Bonazzi, D, Julien, J-D, Romao, M, Seddiki, R, Piel, M, Boudaoud, A, and Minc, N (2014). Symmetry Breaking in Spore Germination Relies on an Interplay between Polar Cap Stability and Spore Wall Mechanics. Developmental Cell 28, 534–546.

7. Butler, YX, Abhayawardhane, Y, and Stewart, GC (1993). Amplification of the Bacillus subtilis maf gene results in arrested septum formation. J Bacteriol 175, 3139–3145.

8. Cortés, JCG, Carnero, E, Ishiguro, J, Sánchez, Y, Durán, A, and Ribas, JC (2005). The novel fission yeast (1,3)β-D-glucan synthase catalytic subunit Bgs4p is essential during both cytokinesis and polarized growth. Journal of Cell Science 118, 157–174.

9. Cortés, JCG, Sato, M, Muñoz, J, Moreno, MB, Clemente-Ramos, JA, Ramos, M, Okada, H, Osumi, M, Durán, A, and Ribas, JC (2012). Fission yeast Ags1 confers the essential septum strength needed for safe gradual cell abscission. Journal of Cell Biology 198, 637–656.

10. De Medina-Redondo, M, Arnáiz-Pita, Y, Clavaud, C, Fontaine, T, Del Rey, F, Latgé, JP, and Vázquez De Aldana, CR (2010). β(1,3)-Glucanosyl-Transferase Activity Is Essential for Cell Wall Integrity and Viability of Schizosaccharomyces pombe. PLoS ONE 5, e14046.

11. De Medina-Redondo, M, Arnáiz-Pita, Y, Fontaine, T, Del Rey, F, Latgé, JP, and De Aldana, CRV (2008). The β-1,3-glucanosyltransferase gas4p is essential for

ascospore wall maturation and spore viability in *Schizosaccharomyces pombe*. Molecular Microbiology 68, 1283–1299.

12. Dekker, N, Van Rijssel, J, Distel, B, and Hochstenbach, F (2007). Role of the α-glucanase Agn2p in ascus-wall endolysis following sporulation in fission yeast. Yeast 24, 279–288.

13. Egel, R (1977). Frequency of mating-type switching in homothallic fission yeast. Nature 266, 172–174.

14. Egel, R, Beach, DH, and Klar, AJ (1984). Genes required for initiation and resolution steps of mating-type switching in fission yeast. Proc Natl Acad Sci USA 81, 3481–3485.

15. Egel, R, and Gutz, H (1981). Gene activation by copy transposition in mating-type switching of a homothallic fission yeast. Curr Genet 3, 5–12.

16. Encinar Del Dedo, J, Dueñas, E, Arnáiz, Y, Del Rey, F, and Vázquez De Aldana, CR (2009). β-Glucanase Eng2 Is Required for Ascus Wall Endolysis after Sporulation in the Fission Yeast *Schizosaccharomyces pombe*. Eukaryot Cell 8, 1278–1286.

17. Escorcia, W, Tripathi, VP, Yuan, J-P, and Forsburg, SL A visual atlas of meiotic protein dynamics in living fission yeast.

18. Frankl, A, Mari, M, and Reggiori, F Electron microscopy for ultrastructural analysis and protein localization in Saccharomyces cerevisiae. Microb Cell 2, 412–428.

19. Free, SJ (2013). Chapter Two - Fungal Cell Wall Organization and Biosynthesis. In: Advances in Genetics, ed. T Friedmann, JC Dunlap, and SF Goodwin, Academic Press, 33–82.

20. Fukunishi, K, Miyakubi, K, Hatanaka, M, Otsuru, N, Hirata, A, Shimoda, C, and Nakamura, T (2014). The fission yeast spore is coated by a proteinaceous surface layer comprising mainly Isp3. MBoC 25, 1549–1559.

21. Galichet, A, Sockalingum, GD, Belarbi, A, and Manfait, M (2001). FTIR spectroscopic analysis of *Saccharomyces cerevisiae* cell walls: study of an anomalous strain exhibiting a pink-colored cell phenotype. FEMS Microbiology Letters 197, 179–186.

22. García, I, Tajadura, V, Martín, V, Toda, T, and Sánchez, Y (2006). Synthesis of α-glucans in fission yeast spores is carried out by three α-glucan synthase paralogues, Mok12p, Mok13p and Mok14p. Molecular Microbiology 59, 836–853.

23. Garg, A, Sanchez, AM, Miele, M, Schwer, B, and Shuman, S (2023). Cellular responses to long-term phosphate starvation of fission yeast: Maf1 determines fate

choice between quiescence and death associated with aberrant tRNA biogenesis. Nucleic Acids Research 51, 3094–3115.

24. Gietz, RD, Schiestl, RH, Willems, AR, and Woods, RA (1995). Studies on the transformation of intact yeast cells by the LiAc/SS-DNA/PEG procedure. Yeast 11, 355–360.

25. Gow, NAR, Latge, J-P, and Munro, CA (2017). The Fungal Cell Wall: Structure, Biosynthesis, and Function. Microbiology Spectrum 5, 10.1128/microbiolspec.funk-0035–2016.

26. Griffiths, PR (1983). Fourier Transform Infrared Spectrometry. Science 222, 297–302.

27. Grun, CH (2004). The structure of cell wall -glucan from fission yeast. Glycobiology 15, 245–257.

28. Hatanaka, M, and Shimoda, C (2001). The cyclic AMP/PKA signal pathway is required for initiation of spore germination inSchizosaccharomyces pombe. Yeast 18, 207–217.

29. Hirata, A, and Shimoda, C (1994). Structural modification of spindle pole bodies during meiosis II is essential for the normal formation of ascospores in *Schizosaccharomyces pombe* : Ultrastructural analysis of *spo* mutants. Yeast 10, 173–183.

30. Hochstenbach, F, Klis, FM, van den Ende, H, van Donselaar, E, Peters, PJ, and Klausner, RD (1998). Identification of a putative alpha-glucan synthase essential for cell wall construction and morphogenesis in fission yeast. Proceedings of the National Academy of Sciences 95, 9161–9166.

31. Hoffman, CS, Wood, V, and Fantes, PA (2015). An Ancient Yeast for Young Geneticists: A Primer on the Schizosaccharomyces pombe Model System. Genetics 201, 403–423.

32. Horisberger, M, Vonlanthen, M, and Rosset, J (1978). Localization of α-galactomannan and of wheat germ agglutinin receptors inSchizosaccharomyces pombe. Arch Microbiol 119, 107–111.

33. Humbel, BM, Konomi, M, Takagi, T, Kamasawa, N, Ishijima, SA, and Osumi, M (2001). *In situ* localization of β-glucans in the cell wall of *Schizosaccharomyces pombe*. Yeast 18, 433–444.

34. Hunter, N (2015). Meiotic Recombination: The Essence of Heredity. Cold Spring Harb Perspect Biol, a016618.

35. Imada, K, and Nakamura, T (2016). The exocytic Rabs Ypt3 and Ypt2 regulate the early step of biogenesis of the spore plasma membrane in fission yeast. MBoC 27, 3317–3328.

36. Ishiguro, J, Saitou, A, Durán, A, and Ribas, JC (1997). cps1+, a Schizosaccharomyces pombe gene homolog of Saccharomyces cerevisiae FKS genes whose mutation confers hypersensitivity to cyclosporin A and papulacandin B. J Bacteriol 179, 7653–7662.

37. Jin, J, Wu, R, Zhu, J, Yang, S, Lei, Z, Wang, N, Singh, VK, Zheng, J, and Jia, Z (2015). Insights into the Cellular Function of YhdE, a Nucleotide Pyrophosphatase from Escherichia coli. PLoS ONE 10, e0117823.

38. Jin, Q-W, and McCollum, D (2003). Scw1p Antagonizes the Septation Initiation Network To Regulate Septum Formation and Cell Separation in the Fission Yeast *Schizosaccharomyces pombe*. Eukaryot Cell 2, 510–520.

39. JMichell, A, and Sourfield, G (1970). An Assessment of Infrared Spectra as Indicators of Fungal Cell Wall Composition. Aust Jnl Of Bio Sci 23, 345.

40. Jongebloed, WL, Stokroos, I, Van der Want, JJ, and Kalicharan, D (1999). Non-coating fixation techniques or redundancy of conductive coating, low kV FE-SEM operation and combined SEM/TEM of biological tissues. J Microsc 193, 158–170.

41. Kassem, A, Abbas, L, Coutinho, O, Opara, S, Najaf, H, Kasperek, D, Pokhrel, K, Li, X, and Tiquia-Arashiro, S (2023). Applications of Fourier Transform-Infrared spectroscopy in microbial cell biology and environmental microbiology: advances, challenges, and future perspectives. Front Microbiol 14, 1304081.

42. Kümmerle, M, Scherer, S, and Seiler, H (1998). Rapid and Reliable Identification of Food-Borne Yeasts by Fourier-Transform Infrared Spectroscopy. Appl Environ Microbiol 64, 2207–2214.

43. Lam, I, and Keeney, S (2015). Mechanism and Regulation of Meiotic Recombination Initiation. Cold Spring Harb Perspect Biol 7, a016634.

44. Leupold, U (1958). Studies on Recombination in Schizosaccharomyces pombe. Cold Spring Harbor Symposia on Quantitative Biology 23, 161–170.

45. Liu, J, Tang, X, Wang, H, and Balasubramanian, M Bgs2p, a 1,3-L-glucan synthase subunit, is essential for maturation of ascospore wall in Schizosaccharomyces pombe.

46. Liu, J, Wang, H, McCollum, D, and Balasubramanian, MK (1999). Drc1p/Cps1p, a 1,3-β-Glucan Synthase Subunit, Is Essential for Division Septum Assembly in Schizosaccharomyces pombe. Genetics 153, 1193–1203.

47. López Hernández, JF, Helston, RM, Lange, JJ, Billmyre, RB, Schaffner, SH, Eickbush, MT, McCroskey, S, and Zanders, SE (2021). Diverse mating phenotypes impact the spread of wtf meiotic drivers in Schizosaccharomyces pombe. eLife 10, e70812.

48. Maeda, Y, Kashiwazaki, J, Shimoda, C, and Nakamura, T (2009). The *Schizosaccharomyces pombe* Syntaxin 1 Homolog, Psy1, Is Essential in the Development of the Forespore Membrane. Bioscience, Biotechnology, and Biochemistry 73, 339–345.

49. Manners, DJ, and Meyer, MT (1977). The molecular structures of some glucans from the cell walls of *Schizosaccharomyces pombe*. Carbohydrate Research 57, 189–203.

50. Martín, V, García, B, Carnero, E, Durán, A, and Sánchez, Y (2003). Bgs3p, a Putative 1,3-β-Glucan Synthase Subunit, Is Required for Cell Wall Assembly in Schizosaccharomyces pombe. Eukaryotic Cell 2, 159–169.

51. Martín, V, Ribas, JC, Carnero, E, Durán, A, and Sánchez, Y (2000). *bgs2*$^{+}$, a sporulation-specific glucan synthase homologue is required for proper ascospore wall maturation in fission yeast. Molecular Microbiology 38, 308–321.

52. Matsuo, Y, Tanaka, K, Matsuda, H, and Kawamukai, M (2005). *cda1*$^{+}$, encoding chitin deacetylase is required for proper spore formation in *Schizosaccharomyces pombe*. FEBS Letters 579, 2737–2743.

53. Matsuo, Y, Tanaka, K, Nakagawa, T, Matsuda, H, and Kawamukai, M Genetic Analysis of chs1þ and chs2þ Encoding Chitin Synthases from Schizosaccharomyces pombe.

54. Minasov, G, Teplova, M, Stewart, GC, Koonin, EV, Anderson, WF, and Egli, M (2000). Functional implications from crystal structures of the conserved *Bacillus subtilis* protein Maf with and without dUTP. Proc Natl Acad Sci USA 97, 6328–6333.

55. Miyata, H, and Miyata, M (1981). Mode of conjugation in homothallic cells of Schizosaccharomyces pombe. J Gen Appl Microbiol 27, 365–371.

56. Muñoz, J, Cortés, JCG, Sipiczki, M, Ramos, M, Clemente-Ramos, JA, Moreno, MB, Martins, IM, Pérez, P, and Ribas, JC (2013). Extracellular cell wall β(1,3)glucan is required to couple septation to actomyosin ring contraction. Journal of Cell Biology 203, 265–282.

57. Nakamura, T, Abe, H, Hirata, A, and Shimoda, C (2004). ADAM Family Protein Mde10 Is Essential for Development of Spore Envelopes in the Fission Yeast *Schizosaccharomyces pombe*. Eukaryot Cell 3, 27–39.

58. Nakamura, T, Nakamura-Kubo, M, Hirata, A, and Shimoda, C (2001). The Schizosaccharomyces pombe spo3 +Gene Is Required for Assembly of the Forespore Membrane and Genetically Interacts with psy1 +-encoding Syntaxin-like Protein. MBoC 12, 3955–3972.

59. Nakamura-Kubo, M, Hirata, A, Shimoda, C, and Nakamura, T (2011). The fission yeast pleckstrin homology domain protein Spo7 is essential for initiation of forespore membrane assembly and spore morphogenesis. MBoC 22, 3442–3455.

60. Ohtsuka, H, Imada, K, Shimasaki, T, and Aiba, H (2022a). Sporulation: A response to starvation in the fission yeast *Schizosaccharomyces pombe*. MicrobiologyOpen 11, e1303.

61. Ohtsuka, H, Imada, K, Shimasaki, T, and Aiba, H (2022b). Sporulation: A response to starvation in the fission yeast *Schizosaccharomyces pombe*. MicrobiologyOpen 11, e1303.

62. Okuzaki, D, Satake, W, Hirata, A, and Nojima, H (2003). Fission yeast meu14+ is required for proper nuclear division and accurate forespore membrane formation during meiosis II. Journal of Cell Science 116, 2721–2735.

63. Onishi, M, Iida, M, Koga, T, Yamada, S, Hirata, A, Iwaki, T, Takegawa, K, Fukui, Y, and Tachikawa, H (2007). *Schizosaccharomyces pombe* Sst4p, a Conserved Vps27/Hrs Homolog, Functions Downstream of Phosphatidylinositol 3-Kinase Pik3p To Mediate Proper Spore Formation. Eukaryot Cell 6, 2343–2353.

64. van Opijnen, T, Bodi, KL, and Camilli, A (2009). Tn-seq: high-throughput parallel sequencing for fitness and genetic interaction studies in microorganisms. Nat Methods 6, 767–772.

65. Osumi, M, Sato, M, Ishijima, SA, Konomi, M, Takagi, T, and Yaguchi, H (1998). Dynamics of Cell Wall Formation in Fission Yeast,Schizosaccharomyces pombe. Fungal Genetics and Biology 24, 178–206.

66. Peat, S, Whelan, WJ, and Edwards, TE (1961). 6. Polysaccharides of baker's yeast. Part IV. Mannan. J Chem Soc, 29–34.

67. Pérez, P, Cortés, JCG, Cansado, J, and Ribas, JC (2018). Fission yeast cell wall biosynthesis and cell integrity signalling. The Cell Surface 4, 1–9.

68. Ragni, E, Fontaine, T, Gissi, C, Latgè, JP, and Popolo, L (2007). The Gas family of proteins of Saccharomyces cerevisiae: characterization and evolutionary analysis. Yeast 24, 297–308.

69. Schindelin, J, Arganda-Carreras, I, Frise, E, Kaynig, V, Longair, M, Pietzsch, T, Preibisch, S, Rueden, C, Saalfeld, S, Schmid, B, *et al*. (2012). Fiji: an open-source platform for biological-image analysis. Nat Methods 9, 676–682.

70. Shigehisa, A, Okuzaki, D, Kasama, T, Tohda, H, Hirata, A, and Nojima, H (2010). Mug28, a Meiosis-specific Protein of *Schizosaccharomyces pombe* , Regulates Spore Wall Formation. MBoC 21, 1955–1967.

71. Shimoda, C (2004). Forespore membrane assembly in yeast: coordinating SPBs and membrane trafficking. Journal of Cell Science 117, 389–396.

72. Smith, GR (2009). Genetic analysis of meiotic recombination in Schizosaccharomyces pombe. Methods Mol Biol 557, 65–76.

73. Tahara, YO, Miyata, M, and Nakamura, T (2020). Quick-Freeze, Deep-Etch Electron Microscopy Reveals the Characteristic Architecture of the Fission Yeast Spore. JoF 7, 7.

74. Tchigvintsev, A, Tchigvintsev, D, Flick, R, Popovic, A, Dong, A, Xu, X, Brown, G, Lu, W, Wu, H, Cui, H, *et al*. (2013). Biochemical and Structural Studies of Conserved Maf Proteins Revealed Nucleotide Pyrophosphatases with a Preference for Modified Nucleotides. Chemistry & Biology 20, 1386–1398.

75. Tougan, T, Chiba, Y, Kakihara, Y, Hirata, A, and Nojima, H (2002). Meu10 is required for spore wall maturation in *Schizosaccharomyces pombe*. Genes to Cells 7, 217–231.

76. Vyas, A, Freitas, AV, Ralston, ZA, and Tang, Z (2021). Fission Yeast Schizosaccharomyces pombe: A Unicellular “Micromammal” Model Organism. Curr Protoc 1, e151.

77. Yamamoto, A, West, RR, McIntosh, JR, and Hiraoka, Y (1999). A Cytoplasmic Dynein Heavy Chain Is Required for Oscillatory Nuclear Movement of Meiotic Prophase and Efficient Meiotic Recombination in Fission Yeast. The Journal of Cell Biology 145, 1233–1250.

78. Yamaoka, T, Imada, K, Fukunishi, K, Yamasaki, Y, Shimoda, C, and Nakamura, T (2013). The Fission Yeast Synaptobrevin Ortholog Syb1 Plays an Important Role in Forespore Membrane Formation and Spore Maturation. Eukaryotic Cell 12, 1162–1170.

79. Yoo, BY, Calleja, GB, and Johnson, BF (1973). Ultrastructural changes of the fission yeast (Schizosaccharomyces pombe) during ascospore formation. Archiv Mikrobiol 91, 1–10.

80. Zuiderveld, K (1994). Contrast limited adaptive histogram equalization. In: Graphics Gems IV, USA: Academic Press Professional, Inc., 474–485.